Investigation of Ligand Protected Gold Clusters on Defect Rich ALD Titania using Electron Spectroscopies

Thesis presented to the College of Chemical and Physical sciences, College of Science and Engineering of Flinders University in candidacy for the degree of

Master of Science by Research

25 July 2018

Gowri Krishnan

Table of Contents

Abstract

The use of sunlight for the photocatalytic conversion of carbon dioxide into useful chemical fuels has gained attention in recent years. The high photocatalytic activity can be achieved with help of the efficient heterogeneous photo catalyst in which the catalyst possesses a different state of matter (gas, liquid and solid) compared to the reactant or products. Gold nanoclusters in few nanometre dimensions exhibit distinct electronic properties with the change in the size of the clusters. These discrete properties make them unique for photocatalytic applications. Titania is a widely used metal oxide support for heterogeneous catalysis. The pre-treatment of the substrate plays a critical role in the photocatalytic reactions and helps in the strong attachment of the nanoclusters with the substrate which results in high catalytic activity.

In this research, atomically precise chemically synthesised ligand protected gold cluster were used as the metal nanoclusters. The chemically synthesised gold nanoclusters are protected by the triphenylphosphine ligands and therefore the size of the cluster is controlled. The atomic layer deposition (ALD) titania was employed as the metal oxide support as it has a flat uniform surface making it suitable for surface studies. The pre-treatment of the ALD titania was performed by heating to remove hydrocarbons and sputtering to create oxygen vacancies prior to the deposition of the gold nanoclusters onto the surface of the ALD titania. The deposition of the chemically synthesised clusters onto the surface of the titania was performed by the solution-based deposition method. The triphenylphosphine ligands were removed by heat treatment in ultra-high vacuum at 200°C for 20 minutes thus creating contact of the gold nanoclusters with the substrate. The interaction of the gold nanoclusters with the titania substrate can be studied with a combination of the surface analytical techniques such as Metastable Induced Electron Spectroscopy (MIES), X-ray Photoelectron Spectroscopy (XPS), Ultraviolet Photoelectron Spectroscopy (UPS) and Inverse Photoemission Spectroscopy (IPES). In this research, ALD titania was used as the metal oxide substrate which has the flat uniform surface makes it beneficial for the surface studies. Metastable Induced Electron Spectroscopy (MIES) is an extreme surface sensitive analytical technique used to study the

outermost valence electronic structure of the sample surface. X-ray Photoelectron Spectroscopy (XPS) is used to study the chemical composition of the sample surface. The Ultraviolet Photoelectron Spectroscopy (UPS) and Inverse photoemission spectroscopy (IPES) are used to study the valence and conduction band electronic structure. Thus, the combination of the Ultraviolet Photoelectron Spectroscopy (UPS) and Inverse Photoemission Spectroscopy (IPES) gives the complete band structure of the sample surface.

Declaration

I certify that this thesis does not incorporate without acknowledgment any material previously submitted for a degree or diploma in any university and that to the best of my knowledge and belief it does not contain any material previously published or written by another person except where due reference is made in the text.

Gowri Krishnan

Acknowledgement

First of all, I would like to thank my Supervisor Professor Gunther Andersson for his kind and invaluable support throughout my study. I'm grateful to work with such a dedicated person and he has been the inspiration for me. His moral support and encouragement helped me to gain the confidence and progress well in my studies.

I would like to thank Dr.Vladimir Golovko, University Of Canterbury, Christ church, New Zealand for providing me with the gold clusters and Professor Greg Metha and his group, University of Adelaide, South Australia for the DFT calculations.

Also, I would like to Namsoon Eom, PHD candidate (ANU) for helping me with the fabrication of the ALD titania.

I would like to extend my thanks to the Gunther's group for their guidance and support throughout my project.

I would like to acknowledge the funding sources (DFEEST scholarship) for my Master's degree.

Lastly, special thanks to my family for their love and encouragement during this journey.

Gowri Krishnan

Flinders University

List of Publications

1. Krishnan, G.; Al Qahtani, H. S.; Li, J.; Yin, Y.; Eom, N.; Golovko, V. B.; Metha, G. F.; Andersson, G. G., Investigation of Ligand-Stabilized Gold Clusters on Defect-Rich Titania. The Journal of Physical Chemistry C **2017**, 121, 28007-28016.

2. Krishnan, G.; Eom, N.; Golovko, V. B.; Metha, G. F.; Andersson, G. G., Investigation of Ligand-Stabilized $[Au_{13}(PPh_3)_8](NO_3)$ clusters on Defect-Rich Titania using electron spectroscopies. Planned submission to The Journal of Physical Chemistry Letters **2018.**

List of Figures

Abbreviation

XPS	X-ray Photoelectron spectroscopy
MIES	Metastable Induced Electron Spectroscopy
UPS	Ultraviolet Photoelectron Spectroscopy
SVD	Singular Value Decomposition
DOS	Density Of States
UHV	Ultra-High Vacuum
KE	Kinetic Energy
BE	Binding Energy
eV	Electron Volt
TOF	Time Of Flight
FWHM	Full Width Half Maximum
ALD	Atomic Layer Deposition
mM	Millimolar
nm	Nanometer
DFT	Density Functional Theory
IPES	Inverse Photoemission Spectroscopy
TiO_2	Titania
HSA	Hemispherical Analyser

Chapter 1

Introduction

Photo catalysis is the process when light is irradiated onto a semiconductor surface, the excitation of the electrons takes place from the valence band to the conduction band leaving the holes behind and the charge carriers drive a chemical reaction. The energy gap between the valence band and conduction band is called the band gap. The excited electrons and holes from the photocatalytic system take part in reduction and oxidation reactions as shown in equation (1) and (2). The oxidation and reduction reactions mentioned below is an example of water splitting reaction.

Oxidation reaction:

$2H_2O \rightarrow O_2 + 4H^+ + 4e^-$ ……..……. (1)

Reduction reaction:

$2H_2O + 2e^- \rightarrow H_2 + 2OH^-$ …….……..… (2)

Heterogeneous catalysis is the process in which the catalyst and reactants/products have a different form of state such as solid, liquid or gas. The metal oxide substrate is found favourable for the heterogeneous catalytic process. The Titanium dioxide (TiO_2) is a widely used semiconductor material for the photocatalytic applications.[1] The catalytic activity of TiO_2 was further enhanced with the metal nanoclusters as the heterogeneous catalyst.[2-3] The use of efficient catalyst has gained attraction in the photocatalytic applications.[4] In heterogeneous catalysis, the catalyst helps in separation of the charges (electrons and holes) on excitation with the light thus speeding up the redox reactions thus increasing the conversion efficiency of the photocatalytic system. The study of the interface between the catalyst and the substrate helps with the selection of an efficient catalyst and a better understanding of the mechanism of heterogeneous catalysis.

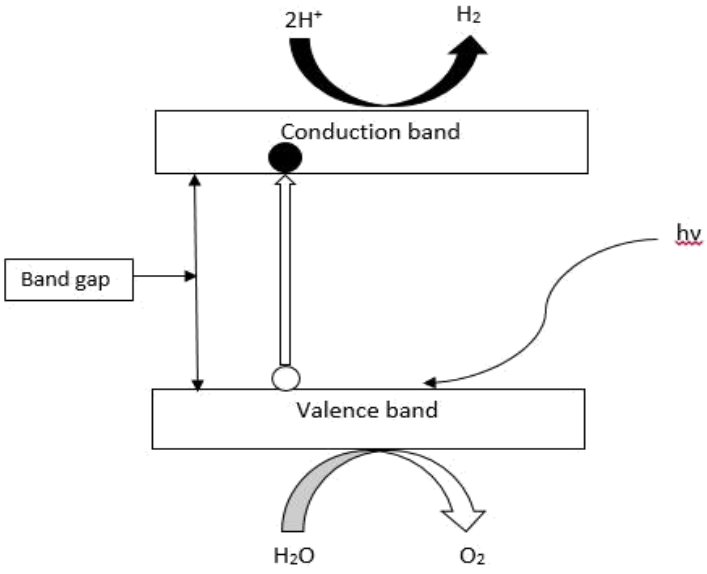

Figure 1.1: Illustrates the excitation of electron from the valence band to conduction band leaving holes behind.

Metal nanoclusters possess a size that lies in between that of single atoms and metal nanoparticles. These small sized metal nanoclusters are gaining attention in recent years due to their electronic properties changing with the addition or removal of single atoms from the nanoclusters. The change of the electronic properties changes the catalytic behaviour. [5-6] This makes nanoclusters unique for photocatalytic applications. In contrast, bulk gold is found to be non-reactive in the same chemical environment. Gold nanoclusters with a few nanometre dimensions are found to be active for the number of photocatalytic reactions like water splitting, hydrogenation, CO oxidation.[7-9] The synthesis/fabrication of the nanoclusters takes place in specific system setup environment and can be classified into two different methods: gas phase and chemical synthesis. In gas phase synthesis, there is a direct contact happens due to the evaporation deposition of the nanoclusters with the surface of the substrate while in case of chemical synthesis, the nanoclusters are protected by the ligands in which the size of the clusters can be controlled by changing the parameters. The ligands protecting the surface of the clusters can be removed by heat treatment in UHV depending on the type of ligands (e.g. S-based ligands are hard to remove via heating)[10] thus providing the contact with substrate. The catalytic activity relies on the nature of the substrate, size and electronic properties of the clusters and the interaction of cluster with the substrate.[11,12] The role of the clusters in the catalytic process are such that the discrete electronic states of the clusters could be useful to modify the band gap in Figure 1. The modification is dependent on the number of atoms forming the cluster. Therefore, it is important to study the density of states of the surface. Another property of the clusters is that they change their geometric configuration easily

(dynamic fluxionality). It is speculated that this together with the ability to attract molecules like water to the cluster makes them reactive.[13]

Titania is the most widely used material for the photocatalytic process due to its moderate stability in acidic and chemical environment, low toxicity and strong bonding with metals.[2,14] The catalytic experiments were performed earlier with different size of gold clusters on various metal oxide supports. The number of gold atoms influences the electronic structure and the chemical activity of the metal oxide support surface.[15] The chemical activity is determined by the charge transfer from the oxide support to the metal nanoclusters. Titania was found to be a suitable substrate for heterogeneous based catalysis. Gold catalyst around 2nm diameter on the titania surface have been found to be catalytically active for CO oxidation at low temperature by Goodman and co-workers.[8] Au_7 was found to be chemically inert for CO oxidation while gold clusters (Au_n, n > 8-20) have found to be catalytically active.[16] Au_{10} synthesised via gas phase on rutile TiO_2 support is found to be catalytically active for CO oxidation.[17] Studies have shown that the catalytic activity is greatly influenced by defects on the support surface. Gold on the reducible supports (TiO_2, Co_3O_4, FeO_3) have shown to be more active than non-reducible supports (SiO_2, Al_2O_3).[18] The strong attachment of the metal clusters with the support will help to avoid the agglomeration of the clusters which results in high photocatalytic activity. This can be achieved with the pre-treatment of the support prior to the deposition of the clusters. There are several pre-treatment methods used such as heating,[19-20] oxygen plasma[21] and sputtering.[22-23] The defects like oxygen vacancy act as a favourable site for the attachment of the clusters onto the surface of the substrate thus influencing the density and size of the clusters.[24] Small size clusters of gold (Au_8) on a defect rich MgO surface resulted in CO oxidation when performed at low temperature.[18] Au_{55} clusters regardless of inert supports resulted in enhanced catalytic activity in the selective oxidation of styrene.[20] Gold clusters as the catalyst in combustion reactions on defective and non-defective MgO (100) films studied by varying the number of gold atoms ($n<20$) showed that Au_8 is the smallest catalytically active size.[24] Research has been undertaken previously with chemically synthesised gold clusters onto a titania surface wherein the chemical composition and changes in the oxidation state were observed using the XPS which resulted in un-agglomerated clusters.[25-26] The density of states was studied with chemically synthesised Au_9 clusters on silica and titania surfaces in which the oxygen plasma was used as the pre-treatment method.[27]

In this research, atomically precise chemically synthesised ligand stabilised gold clusters (Au_n, n=9, 13) were deposited onto a pre-treated (heated and sputtered) ALD titania. The ligands must be removed from the surface of the gold clusters in case of the chemical synthesis to make them catalytically active. Also, the strong attachment of the gold clusters to the titania surface avoids the agglomeration of the clusters which would contribute to a high catalytic activity. Thus, the pre-treatment of the titania substrate plays a major role in the catalytic activity. The pre-treatment of the ALD titania was performed by heating and subsequent sputtering. The post heat treatment was done in UHV at 200°C for 20 minutes to remove the ligands protecting the gold clusters. It is important to observe the change in the chemical activity and the density of states which gives a better understanding about the catalyst used in the photocatalytic applications. ALD titania possess a flat and uniform surface which makes it favourable for surface studies. MIES is used to study the electronic structure (DOS) of the outermost layer of the sample and X-ray Photoelectron spectroscopy (XPS) is used to identify the chemical composition of the sample surface and to observe the change in the gold clusters after deposition and post heat treatment.

1.1. References

1. Sanchez, A.; Abbet, S.; Heiz, U.; Schneider, W. D.; Häkkinen, H.; Barnett, R. N.; Landman, U., When Gold Is Not Noble: Nanoscale Gold Catalysts. *The Journal of Physical Chemistry A* **1999**, *103*, 9573-9578.

2. Bagheri, S.; Muhd Julkapli, N.; Bee Abd Hamid, S., Titanium Dioxide as a Catalyst Support in Heterogeneous Catalysis. *The Scientific World Journal* **2014**, *2014*, 21.

3. Chen, M.; Goodman, D. W., Catalytically Active Gold on Ordered Titania Supports. *Chem Soc Rev* **2008**, *37*, 1860-70.

4. Min, B. K.; Wallace, W. T.; Goodman, D. W., Support Effects on the Nucleation, Growth, and Morphology of Gold Nano-Clusters. *Surface Science* **2006**, *600*, L7-L11.

5. Anpo, M., Photocatalysis on Titanium Oxide Catalysts: Approaches in Achieving Highly Efficient Reactions and Realizing the Use of Visible Light. *Catalysis Surveys from Asia* **1997**, *1*, 169-179.

6. Schweinberger, F. F., et al., Cluster Size Effects in the Photocatalytic Hydrogen Evolution Reaction. *Journal of the American Chemical Society* **2013**, *135*, 13262-13265.

7. Wörz, A. S.; Judai, K.; Abbet, S.; Heiz, U., Cluster Size-Dependent Mechanisms of the Co + No Reaction on Small Pdn ($N \leq 30$) Clusters on Oxide Surfaces. *Journal of the American Chemical Society* **2003**, *125*, 7964-7970.

8. Lopez, N., On the Origin of the Catalytic Activity of Gold Nanoparticles for Low-Temperature Co Oxidation. *Journal of Catalysis* **2004**, *223*, 232-235.

9. Choudhary, T. V.; Goodman, D. W., Catalytically Active Gold: The Role of Cluster Morphology. *Applied Catalysis A: General* **2005**, *291*, 32-36.

10. Shimizu, T.; Teranishi, T.; Hasegawa, S.; Miyake, M., Size Evolution of Alkanethiol-Protected Gold Nanoparticles by Heat Treatment in the Solid State. *The Journal of Physical Chemistry B* **2003**, *107*, 2719-2724.

11. Valden, M.; Lai, X.; Goodman, D. W., Onset of Catalytic Activity of Gold Clusters on Titania with the Appearance of Nonmetallic Properties. *Science* **1998**, *281*, 1647-1650.

12. Heiz, U.; Sanchez, A.; Abbet, S.; Schneider, W.-D., The Reactivity of Gold and Platinum Metals in Their Cluster Phase. *The European Physical Journal D - Atomic, Molecular, Optical and Plasma Physics* **1999**, *9*, 35-39.

13. Chen, M. S.; Goodman, D. W., Structure–Activity Relationships in Supported Au Catalysts. *Catalysis Today* **2006**, *111*, 22-33.

14. Jeyalakshmi, V.; Mahalakshmy, R.; Krishnamurthy, K.; Viswanathan, B., Titania Based Catalysts for Photoreduction of Carbon Dioxide: Role of Modifiers. **2012**.

15. Heiz, U.; Vanolli, F.; Sanchez, A.; Schneider, W. D., Size-Dependent Molecular Dissociation on Mass-Selected, Supported Metal Clusters. *Journal of the American Chemical Society* **1998**, *120*, 9668-9671.

16. Grunwaldt, J.-D.; Baiker, A., Gold/Titania Interfaces and Their Role in Carbon Monoxide Oxidation. *The Journal of Physical Chemistry B* **1999**, *103*, 1002-1012.

17. Xing, X.; Yoon, B.; Landman, U.; Parks, J. H., Structural Evolution of Au Nanoclusters: From Planar to Cage to Tubular Motifs. *Physical Review B* **2006**, *74*, 165423.

18. Haruta, M., Size-and Support-Dependency in the Catalysis of Gold. *Catalysis today* **1997**, *36*, 153-166.

19. Turner, M.; Golovko, V. B.; Vaughan, O. P. H.; Abdulkin, P.; Berenguer-Murcia, A.; Tikhov, M. S.; Johnson, B. F. G.; Lambert, R. M., Selective Oxidation with Dioxygen by Gold Nanoparticle Catalysts Derived from 55-Atom Clusters. *Nature* **2008**, *454*, 981-983.

20. Raja, R.; Golovko, V. B.; Thomas, J. M.; Berenguer-Murcia, A.; Zhou, W.; Xie, S.; Johnson, B. F. G., Highly Efficient Catalysts for the Hydrogenation of Nitro-Substituted Aromatics. *Chemical Communications* **2005**, 2026-2028.

21. Boyen, H. G.; Ethirajan, A.; Kästle, G.; Weigl, F.; Ziemann, P.; Schmid, G.; Garnier, M. G.; Büttner, M.; Oelhafen, P., Alloy Formation of Supported Gold Nanoparticles at Their Transition from Clusters to Solids: Does Size Matter? *Physical Review Letters* **2005**, *94*, 016804.

22. Al Qahtani, H. S.; Metha, G. F.; Walsh, R. B.; Golovko, V. B.; Andersson, G. G.; Nakayama, T., Aggregation Behavior of Ligand-Protected Au9 Clusters on Sputtered Atomic Layer Deposition Tio2. *The Journal of Physical Chemistry C* **2017**, *121*, 10781-10789.

23. Krishnan, G.; Al Qahtani, H. S.; Li, J.; Yin, Y.; Eom, N.; Golovko, V. B.; Metha, G. F.; Andersson, G. G., Investigation of Ligand-Stabilized Gold Clusters on Defect-Rich Titania. *The Journal of Physical Chemistry C* **2017**, *121*, 28007-28016.

24. Wallace, W. T.; Min, B. K.; Goodman, D. W., The Stabilization of Supported Gold Clusters by Surface Defects. *Journal of Molecular Catalysis A: Chemical* **2005**, *228*, 3-10.

25. Anderson, D. P., et al., Chemically Synthesised Atomically Precise Gold Clusters Deposited and Activated on Titania. Part Ii. *Phys Chem Chem Phys* **2013**, *15*, 14806-13.

26. Anderson, D. P.; Alvino, J. F.; Gentleman, A.; Qahtani, H. A.; Thomsen, L.; Polson, M. I.; Metha, G. F.; Golovko, V. B.; Andersson, G. G., Chemically-Synthesised, Atomically-Precise Gold Clusters Deposited and Activated on Titania. *Phys Chem Chem Phys* **2013**, *15*, 3917-29.

27. Andersson, G. G., et al., Phosphine-Stabilised Au(9) Clusters Interacting with Titania and Silica Surfaces: The First Evidence for the Density of States Signature of the Support-Immobilised Cluster. *J Chem Phys* **2014**, *141*, 014702.

Chapter 2

Experimental methods

2.1. Photoelectron spectroscopy:

The photoelectron spectroscopy works on the photoelectric effect. When the sample is irradiated with photons, electrons are ejected from the surface of the sample and these electrons are called photoelectrons. The ejected electrons enter the analyser which measures the kinetic energy of the photoelectrons. The relationship between the energy of the incident photon (hν), the kinetic energy (KE) and the binding energy (BE) of the ejected electron is given by the equation,

$BE = h\nu - KE - \Phi$ …….. (1)

Where Φ is the work function of the analyser.

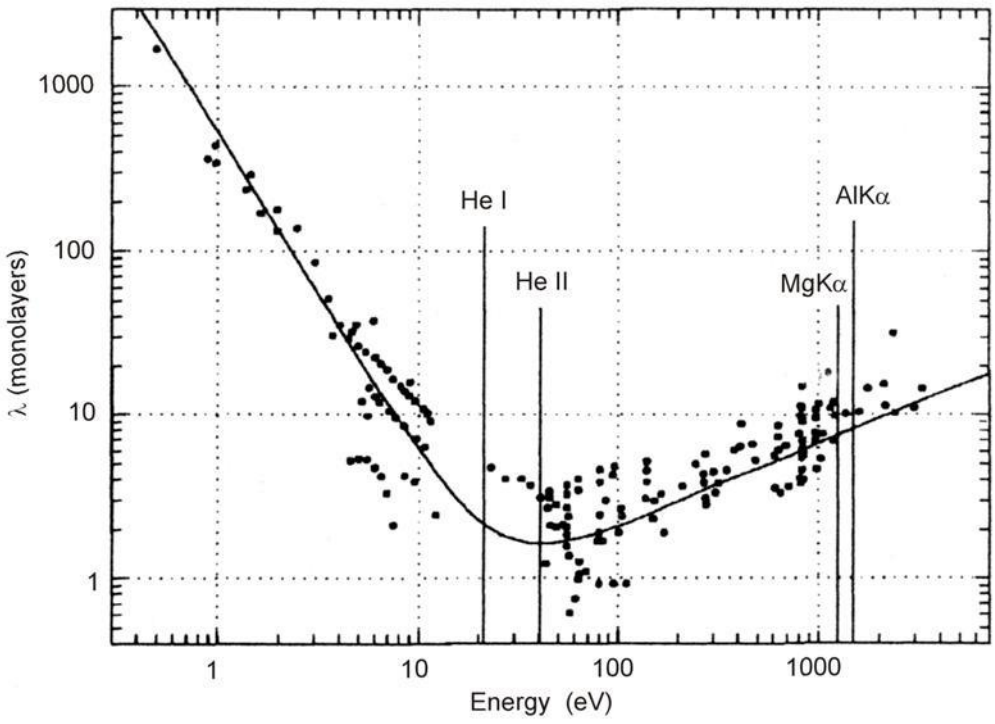

Figure 1.1: Variation in the depth sensitivity of photon spectroscopy vs applied energy.[1]

2.1.1. X-ray Photoelectron spectroscopy (XPS):

X-ray photoelectron spectroscopy is a surface analytical technique used to determine the chemical composition of the sample surface. XPS is operated in an UHV environment with a SPECS PHOIBOS-HSA3500 analyser. The X-ray source used is equipped with a Mg and Al anode. Thus, XPS can be performed with either the MgKα (excitation energy of 1253.6 eV) or the AlKα line (excitation energy of 1486.7 eV). X-rays of high energy is used as the source which results in the emission of electrons from the core of atoms forming the sample. When performing high resolution spectra, the emitted electrons from the sample surface enter the HSA analyser with a pass energy 10eV where the electrons with the sufficient energy pass through the detector which measures the kinetic energy of the emitted electrons. The kinetic energy is then converted into the binding energy using equation 1. The chemical composition of the sample is identified through the binding energy related to the identified peaks in the spectrum. XPS is surface sensitive because approximately only the electrons which are emitted near the surface usually 3(λ) where λ is the electron mean free path depending on the sample (*e.g.* around 1-10 nm deep), contribute to the signal resulting in the XP spectrum (*i.e.*, limited electron mean free path).[3] The surface sensitivity can be explained by the electron intensity attenuated in the bulk. The electron intensity is given by,

$$I\ (d, E, \alpha) = I\text{o}\ \exp(-\frac{d}{\cos(\alpha)}.\lambda(E)) \ldots\ldots\ldots\ldots\ldots\ldots\ldots\ldots\ldots\ldots\ldots\ldots\ldots\ldots\ldots\ldots\ldots\ldots\ldots\ldots \quad (2)$$ [2]

Where d is the depth, I_0 is the primary intensity, I is the intensity, α(=90°) is the angle between the direction to the detector and the surface normal, $\lambda(E)$is the electron mean free path which depends on the kinetic energy of the electrons.

The Shirley background has a certain slope which can be adjusted to fit the background signal from electron scattering. The Lorentz (30%) and Gaussian (70%) function contributes to the peak fitting which gives the intrinsic line shape of the peak.

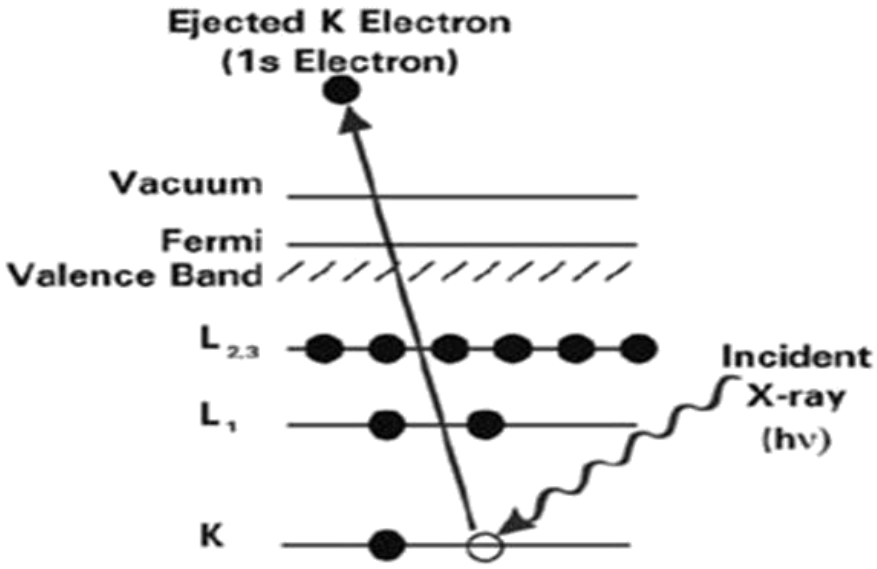

Figure 2.2: The excitation of core electrons with incident x-rays.[3]

2.1.2. Metastable Induced Electron Spectroscopy (MIES):

MIES is a surface sensitive analytical technique used to determine the electronic structure of the outermost layer of the sample. The two stage cold cathode gas discharge is used as the source which generates metastable helium atoms mainly in the $^3S1$ state (19.8 eV) and photons (21.2 eV) simultaneously.[4] A mechanical chopper with a frequency of 2000Hz is used to separate the signals of the emitted electrons due to the impact of UV photons and He* with the time of flight (TOF) technique. MIES is extremely surface sensitive because the metastable helium atoms release their energy to the surface at a distance of just a few Å *via* two mechanisms. The first mechanism is resonant ionization (RI) followed by Auger neutralization (AN) while the second mechanism is Auger de-excitation (AD).[5-8] The mechanism is dependent on the electronic structure of the surface and work function of the sample. The RI and AN takes place in case of the low work function of the sample. The resonant ionization happens when the 2s electron from the helium metastable atom imparts its energy to the sample surface resulting in a positive helium ion. The electrons from the surface of the sample tunnels into the 1s orbital which neutralizes the helium ion, so called Auger neutralization. The RI and AN processes results in the broadening of the spectrum. The Auger de-excitation takes place in case of low band gap materials and results in a spectrum with the sharp features. The kinetic energy of the emitted electrons is measured with a hemispherical analyser, which gives the spectrum showing a number of electrons escaping from the surface of the sample with various kinetic energies.

The energy relation is given by,

$E_{bin} = E_{excitation}(He^*) - E_{kin} - \Phi_{spec}$ …….. (3)

Where E_{bin} is the binding energy of the electron, $E_{excitation}(He^*)$ is the excitation energy of the helium atom, Φ_{spec} is the spectrometer work function (constant), E_{kin} is the kinetic energy of the electron. Equation (3) holds only for the Auger de-excitation process. The measured MIES spectrum is analysed using the singular value decomposition algorithm.[31] In general, it is not possible to obtain the reference spectrum for the species that exist on its own. For example, the gold clusters doesn't exist without the presence of ligands. Therefore, SVD algorithm was used to determine the reference spectrum which doesn't exist independently. The SVD algorithm follows three main steps: the first step is a mathematical procedure used to determine the number of individual vectors which defines the number of base spectra required to fit the measured MIES spectra. The base spectra obtained from the mathematical procedure doesn't have to be physically meaningful. The number of base spectra is equal to the number of reference spectra. The two main criterions in defining meaningful reference spectra are (i) the reference spectra should be non-negative and (ii) the sum of the weighting factors should be less than or equal to zero.

2.1.3. Inverse Photoemission Spectroscopy (IPES):

Inverse photoelectron spectroscopy is a surface analytical technique used to determine the unoccupied density of states at the surface of a sample. IPES provides information about the unoccupied electronic states between the Fermi and vacuum level. IPES works on the electron in and photon out mechanism, from which the photoemission is performed in a reversed mode. The technique directs electrons with well-defined energy onto a sample related to the equilibrated Fermi level of the sample by a Ta_2O filament electron gun. The electrons are absorbed by the sample and make a transition to the unoccupied states via emission of a photon. The energy of the photon is measured and allows the determination of the energy of the unoccupied state. The photon detector consists of an UV band pass filter photon[10] which allows the selective UV spectral bands to transmit thus avoiding the band signals which are out of wavelength range. The photon detector is operated in the isochromatic detecting mode with the Geiger Mueller tube filled with acetone embodied in Ar gas and used as the ionizing gas detector with a photon energy of ~7.9 eV. The IPES spectrum is composed of photons detected as a function of the kinetic energy of the incident electron beam. The spectrum energy offset can be identified as the occurrence of the conductive band (CB). Thus, the complete energy band structure of a sample up to a depth of a few nanometres including measurement of the work function can studied with a combination of IPES and UPS.

2.2 Computational Method:

The theoretical calculations were performed by Junda Li (University of Adelaide). For the calculation of the geometry and electronic structure of Au_9/TiO_2 the plane-wave basis set DFT code Vienna ab initio simulation package was used.[11-12] Interaction between core and valence electrons is described by the projector augmented wave (PAW) approach.[13] The Perdew-Burke-Ernzerhof (PBE) [14] GGA exchange-correlation functional was used in the calculations. Total energy and volume scans of bulk anatase TiO_2 unit cell were initially computed using a plane wave cut-off of 475 eV and a Monkhorst-Pack grid of (7x7x3) k-points. The equilibrium lattice parameters were calculated by fitting to the Murnaghan equation of state, which gave the values of a=3.779 Å and c=9.473 Å (compared to experimental lattice parameters a=3.784 Å, c=9.514 Å). The optimized unit cell was used to construct a stoichiometric 4×4×2 supercell (101) surface slab. In order to eliminate slab-slab interaction a vacuum space of 20 Å was added above the surface, which was sufficiently large. The final supercell's lattice parameters were a=21.77 Å, b=15.10 Å, c=30.84 Å, α=β=90, γ=110.30, which were enough to avoid any self-interaction of adsorbed clusters due to periodic boundary condition. The adsorption energy E_{ads} was calculated through,

$$E_{ads} = E_{surf\text{-}ads} - (E_{surf} + E_{ads}) \quad (4)$$

where $E_{surf\text{-}ads}$ is the energy of the surface with the adsorbate attached, E_{surf} the energy of the anatase (101) surface and E_{ads} the energy of the isolated adsorbate. The settings for the supercell calculations are as follow: The convergent standards were set to 10-6 eV for the self-consistent field (SCF), 0.03 eV/ Å for the maximum force for the geometry optimization. Due to the large supercell, only the gamma point was included for k-points grid sampling during the geometry optimization.

In order to calculate the density of states (DOS), the k-points grid was increased to a gamma-centred 2×2×2 Monkhorst-Pack grid, which resulted in 8 irreducible k-points in the first Brillouin zone. The projected-DOS (PDOS) were calculated by projecting the wave functions onto spherical harmonics centred on the atoms with radii of 1.5 Å. The localized-PDOS (LPDOS) was calculated by only including the top layer of the TiO_2 surface (~2 Å depth) as well as all Au_9 atoms. Note that the calculation is equivalent to a % mass loading of Au: TiO_2 of 35%.

2.3. Material and sample preparation:

ALD titania was fabricated by depositing a thin layer of titania on a P Type B-doped silicon wafer (MTI Corporation, USA) via atomic layer deposition (ALD).The wafers have a resistivity $\leq 0.005\Omega$cm. ALD deposition of titania on the silica wafer resulted in the fabrication of an amorphous titania film with surface roughness (R_{rms}) less than 1 nm, as explained in detail by Walsh *et al.*[15] Applying the ALD process above 180 ºC results in a polycrystalline anatase phase[16] with the thickness of ~5 nm[16,17] and it can be assumed that heating the amorphous ALD titania to similar temperatures results in a similar crystalline structure. The gold nanoclusters were synthesized following the procedure described by Wen *et al.*[18] Methanol (ACI labscan, super gradient HPLC,99.9%) is used as the solvent without additional purification. The ALD titania wafers were cut into 1x1cm pieces and pre-treated by heating and sputtering to obtain a uniform surface for the attachment of Au clusters onto the ALD TiO_2 surface, reproducible composition and titania defect density as will be seen from the results. The details of heating and sputtering will be described in the results section. The result of heating prior to sputtering is to generate a uniform surface before the deposition of Au clusters. The deposition of clusters was performed by immersing the pre-treated ALD titania samples in methanol solutions of Au_n (n=9,13) (ranging in concentration from 0.0001 mM up to 0.06 mM) for 30 minutes, followed by rinsing (quick dip) with pure methanol and blow drying with dry nitrogen. For example, 0.06 mM Au_n cluster solution is prepared by dissolving 0.54 mg of Au_n in 1.98 mL of methanol. The Au_n clusters deposited on ALD titania were heat-treated (post-treatment) under ultra-high vacuum (10^{-9} mbar) at 200°C for 20 minutes to remove the ligands protecting the gold clusters. The above conditions for the post treatment are based on our previous results from heating and sputtering of the ALD titania substrate.[19]

2.3.1. Cluster preparation method:

The clusters were synthesized by Vladimir Golovko (University of Canterbury) according to the protocol as explained by Wen et al.[20] The mixture of $NaBH_4$ and ethanol was added to the Au (PPh_3) NO_3 and ethanol mixture and dried in the atmospheric air for 2 hours. The resulting dark brown filtrate was dried in vacuo and dissolved in methylene dichloride. After filtration and solvent evaporation, the residue was collected, then washed with tetrahydrofuran and hexane to provide the final green powder for Au_9 and purple powder for the Au_{13} clusters. The amount of the chemical mixture differs for the different clusters.

2.4. References

1. Hannu, H.; Stéphane, A.; Antonio, S.; Ulrich, H.; Uzi, L., Structural, Electronic, and Impurity-Doping Effects in Nanoscale Chemistry: Supported Gold Nanoclusters. *Angewandte Chemie International Edition* **2003**, *42*, 1297-1300.

2. The Size of Neutral Free Clusters as Manifested in the Relative Bulk-to-Surface Intensity in Core Level Photoelectron Spectroscopy. *The Journal of Chemical Physics* **2004**, *120*, 345-356.

3. Seah, M. P.; Dench, W. A., Quantitative Electron Spectroscopy of Surfaces: A Standard Data Base for Electron Inelastic Mean Free Paths in Solids. *Surface and Interface Analysis* **1979**, *1*, 2-11.

4. Hollander, J. M.; Jolly, W. L., X-Ray Photoelectron Spectroscopy. *Accounts of Chemical Research* **1970**, *3*, 193-200.

5. Höfft, O.; Bahr, S.; Himmerlich, M.; Krischok, S.; Schaefer, J. A.; Kempter, V., Electronic Structure of the Surface of the Ionic Liquid [Emim][Tf2n] Studied by Metastable Impact Electron Spectroscopy (Mies), Ups, and Xps. *Langmuir* **2006**, *22*, 7120-7123.

6. Chambers, B. A.; Neumann, C.; Turchanin, A.; Gibson, C. T.; Andersson, G. G., The Direct Measurement of the Electronic Density of States of Graphene Using Metastable Induced Electron Spectroscopy. *2D Materials* **2017**, *4*, 025068.

7. Frerichs, M.; Voigts, F.; Maus-Friedrichs, W., Fundamental Processes of Aluminium Corrosion Studied under Ultra High Vacuum Conditions. *Applied Surface Science* **2006**, *253*, 950-958.

8. Andersson, G. G., et al., Phosphine-Stabilised Au(9) Clusters Interacting with Titania and Silica Surfaces: The First Evidence for the Density of States Signature of the Support-Immobilised Cluster. *J Chem Phys* **2014**, *141*, 014702.

9. Berlich, A.; Liu, Y. C.; Morgner, H., Evaporation of Ni and Carbon Containing Species onto Nio/Ni as Case Study for Metal Support Catalysts Investigated by Metastable Induced Electron Spectroscopy (Mies). *Radiation Physics and Chemistry* **2005**, *74*, 201-209.

10. Finazzi, M.; Bastianon, A.; Chiaia, G.; Ciccacci, F., High-Sensitivity Bandpass UV Photon Detector for Inverse Photoemission. Measurement Science and Technology 1993, 4, 234.

11. Kresse, G.; Furthmüller, J., Efficient Iterative Schemes for Ab Initio Total-Energy Calculations Using a Plane-Wave Basis Set. *Phys. Rev. B* **1996**, *54*, 11169-11186.

12. Kresse, G.; Hafner, J., Ab Initio. *Phys. Rev. B* **1994**, *49*, 14251-14269.

13. Kresse, G.; Joubert, D., From Ultrasoft Pseudopotentials to the Projector Augmented-Wave Method. *Phys. Rev. B* **1999**, *59*, 1758-177513.

14. Perdew, J. P.; Burke, K.; Ernzerhof, M., Generalized Gradient Approximation Made Simple. *Phys. Rev. Lett.***1996**, *77*, 3865-3868.

15. Walsh, R. B.; Nelson, A.; Skinner, W. M.; Parsons, D.; Craig, V. S. J., Direct Measurement of Van Der Waals and Diffuse Double-Layer Forces between Titanium Dioxide Surfaces Produced by Atomic Layer Deposition. *The Journal of Physical Chemistry C* **2012**, *116*, 7838-7847.

16. Aarik, J.; Aidla, A.; Uustare, T.; Ritala, M.; Leskelä, M., Titanium Isopropoxide as a Precursor for Atomic Layer Deposition: Characterization of Titanium Dioxide Growth Process. *Appl. Surf. Sci.* **2000**, *161*, 385-395.

17. Ellis-Gibbings, L.; Johansson, V.; Walsh, R. B.; Kloo, L.; Quinton, J. S.; Andersson, G. G., Formation of N719 Dye Multilayers on Dye Sensitized Solar Cell Photoelectrode Surfaces Investigated by Direct Determination of Element Concentration Depth Profiles. *Langmuir* **2012**, *28*, 9431-9439.

18. Wen, F.; Englert, U.; Gutrath, B.; Simon, U., Crystal Structure, Electrochemical and Optical Properties of $[Au_9(PPh_3)_8](No_3)_3$. *Eur. J. Inorg. Chem.***2008**, *2008*, 106-111.

19. Bennett, T.; Adnan, R. H.; Alvino, J. F.; Golovko, V.; Andersson, G. G.; Metha, G. F., Identification of the Vibrational Modes in the Far-Infrared Spectra of Ruthenium Carbonyl Clusters and the Effect of Gold Substitution. *Inorg. Chem.***2014**, *53*, 4340-4349.

20. Wen, F.; Englert, U.; Gutrath, B.; Simon, U., Crystal Structure, Electrochemical and Optical Properties of $[Au_9(PPh_3)_8](NO_3)_3$. *European Journal of Inorganic Chemistry* **2008**, *2008*, 106-1.

Chapter 3

Investigation of ligand stabilized gold clusters on defect rich titania

This chapter is a reformatted version of the paper published in **The Journal of Physical Chemistry C** 2017, 121, 28007-28016.

3.1. Abstract

Chemically synthesized atomically precise gold clusters stabilized by triphenylphosphine ligands $[Au_9(PPh_3)_8](NO_3)_3$ were deposited onto the surface of titania fabricated via atomic layer deposition. The titania surface was pre-treated by heating and sputtering. After deposition of the clusters onto pre-treated titania, the samples were heated at 200ºC for 20 minutes under ultra-high vacuum and subsequently investigated using metastable induced electron spectroscopy to study the electronic structure of the outermost layer of the sample and x-ray photoelectron spectroscopy to determine the chemical composition of the surface of the sample. The former study revealed that two reference spectra are needed to explain the electronic structure of the sample. One reference spectrum is related to the titania substrate while the second spectrum is related to the presence of the Au cluster cores and the ligands removed from the cluster cores. The latter study found that the Au 4*f* peak is shifted to lower binding energy and P 2*p* peak to higher binding energy after heating. These are interpreted in the light of ligand removal and size evolution of Au particles upon heating of the clusters on titania. The important outcome of the present work is that the defects introduced at the ALD titania surface via sputtering and heating strongly reduces the agglomeration of the Au clusters adsorbed to the surface.

3.2. Introduction

Metal nanoclusters are materials with a size intermediate between metallic nanoparticles and single metal atoms. Metal nanoclusters are interesting due to their strongly size-dependent properties since the addition or removal of even a single atom results in the noticeable change in the electronic properties of the clusters.[1] The Au nanoclusters can be fabricated in the gas phase under ultra-high vacuum [2]and synthesised as ligand protected clusters using solution-based chemical processes.[3] Chemically synthesized ligand stabilized clusters are of interest because they are often stable compounds made in large (milligram to gram) quantities with the size of the cluster core controlled *via* choice of synthetic protocol parameters.

The attachment of nanoclusters onto metal oxides changes the properties of the metal oxide surface and these surfaces have been found interesting in several areas of research such as sensors,[4-5] photovoltaics,[6-7] light emitting diodes[8] and photo catalysis.[9-10] An area of research attracting strong interest is photo catalysis where gold nanoclusters are often found to be catalytically active in contrast to the bulk gold analogues.[11] Titania (TiO_2) has been identified as a suitable support for the Au cluster based heterogeneous catalysis.[12] Titania has low toxicity, is stable in moderately acidic and oxidative environments and makes strong bonds with metals.[13] The electronic structure and interaction of Au nanoclusters with titania could potentially influence the catalytic activity of the titania substrate.[14-16] While the present work aims to determine the electronic structure of the clusters deposited and activated on titania surface, potential applications (catalytic performance, sensing *etc.*) of the cluster-modified surface are not explored here.

The presence of extended and point defects, as well as various chemical functionalities on the surface of titania, significantly affects interaction of gold particles with the support.[17-19] Specific treatments of the surface prior to cluster deposition (pre-treatments) can often be used to introduce such defects and/or functionalities and hence can play a critical role in the attachment of clusters onto the surface of the titania. Earlier studies have explored the effects of different pre-treatment methods, for example, use of oxygen plasma for cleaning the surface results in an oxygen rich layer on the surface.[20] Heating is often used to remove the hydrocarbons, water and can also remove Ti-OH groups, while sputtering can remove surface atoms generating point defects.[21] The defects on support have been found to be of importance in the growth and nucleation of clusters thus strongly influencing the size of the clusters *via* deposition by evaporation of Au.[22-23] From these findings, it can be inferred that defects could help in the attachment of clusters onto the metal surface.

Post treatment has to be applied in order to remove the ligands protecting the Au cluster cores and thus providing the option for improved, direct interaction of Au cluster cores with the substrate. Heat treatment in ultra-high vacuum (UHV) is a widely used treatment for removing the ligands from the surface of the clusters.[24-25] However, the higher temperature increases the likelihood of agglomeration of the cluster cores. The strong attachment of clusters to titania could reduce or even fully prevent cluster agglomeration.

The aim of this study is to deposit chemically synthesized atomically precise gold clusters stabilized by triphenylphosphine ligands [$[Au_9(PPh_3)_8](NO_3)_3$] (hereafter referred to as Au_9) onto the pre-treated (*via* heating and sputtering) TiO_2 films made using atomic layer deposition (ALD) and to determine the change in the density of states of the surface due to the presence of the clusters. The ALD titania substrate used here makes it ideal for surface studies due to the smooth and uniform surface. The electronic structure after heat treatment is studied using a combination of the surface analytical techniques of metastable induced electron spectroscopy (MIES) and ultraviolet photoelectron spectroscopy (UPS), while chemical composition and nature of the key species is studied using X-ray photoelectron spectroscopy (XPS). MIES is a very suitable technique to study the electronic properties of the outermost layer of the sample.

3.3. Results and discussion

3.3.1. XPS results

High resolution spectra were recorded for carbon (C 1*s*), titanium (Ti 2*p*), gold (Au 4*f*), phosphorous (P 2*p*), silicon (Si 2*p*), oxygen (O 1*s*) and nitrogen (N 1s). The number of scans was chosen such that the statistical error was sufficiently small. The XPS data were evaluated by fitting the peaks using a Shirley background to remove the background electron scattering thus giving the intrinsic line shape of the peak.[26] The main C peak was set to a binding energy 285 eV and used for calibrating the peak position of all other elements. The source of C is either from triphenylphosphine ligands or adventitious hydrocarbons (present on all samples exposed to air) and in both cases correspond to C-C bonds.

Surface pre-treatment

The surface of ALD titania is pre-treated by heating and subsequent sputtering to both reduce the presence of hydrocarbons on the titania surface and induce O vacancies. The latter are known to provide sites for preferential adsorption of Au.[27] The ALD titania was heated to different temperatures in the range of 200 to 500 °C in order to find the lowest temperature at which the majority of hydrocarbons can be removed through heating under UHV but without creating a large number of heating-induced defects (i.e. Ti^{3}+ and Ti^{2+}) that would otherwise increase the roughness of the titania surface. The qualitative criterion used here was that the Ti^{4+} XPS peak should still be the dominant contributor. The temperature at which the decrease in the amount of C levels off and at which the proportion of heating-induced defects) is still low was chosen as the temperature for the heating procedure. Figure 3.1 shows that heating at 300 °C (for 10 minutes) in UHV meets these criteria and thus was chosen as the heating temperature. The samples were subsequently sputtered with Ar^{+}, which creates O vacancies in a controlled way on the surface of the ALD titania. The O vacancies result in the formation of Ti^{3}+ and Ti^{2}+defect states with the Ti 2*p* peak positions in XP spectra at 457.8 ± 0.1eV and 455.6 ± 0.1eV respectively. A high-resolution Ti 2*p* spectrum is shown in Figure 3.2 with the peaks related to Ti^{4+}, Ti^{3+} and Ti^{2+} indicated. The fraction of Ti^{3+} and Ti^{2+} of the overall Ti XPS intensity are shown in Figure 3.3. A sputter dose of 2×10^{15} ions/cm^{2} was found to produce only a small fraction of Ti^{2+} and was chosen as the dose for all further preparation of the sample surfaces. Creating defects on the titania surface could influence on the structure of the titania and have a significant impact on binding energy and electronic structure via electron transfer to the highly electronegative gold clusters. The sputtering also removes some of the hydrocarbons which remain on the surface after the pre-heat treatment. The amount of hydrocarbon remaining after pre-heat treatment is 5%, which is further reduced to 2% after sputtering. The desired heating and sputtering conditions are somewhat arbitrary since the amount of hydrocarbon to be removed and the percentage of defects to achieve the optimum adsorption of the Au_9 clusters at the surface is not known. Furthermore, defects such as oxygen vacancies will be removed from the sample surface when the sample becomes exposed to air. Figure S2 in the supporting information gives evidence that the defects generated through heating and sputtering decrease by about 50% when the sample is exposed to air for the period of time required to transfer the heated and sputtered sample from the vacuum chamber to the Au cluster solution (~2 minutes).

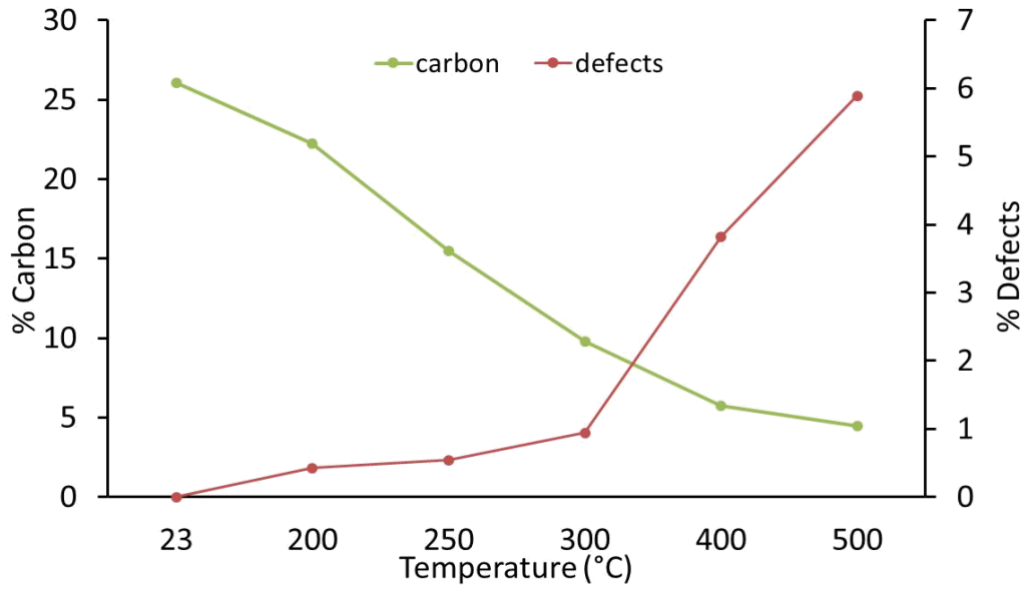

Figure 3.1: Relative amounts of C and TiO_2 defects (sum of Ti^{3+} and Ti^{2+}) as a function of the heating temperature. The relative amount is the fraction of the respective signal as part of the total XPS intensity.

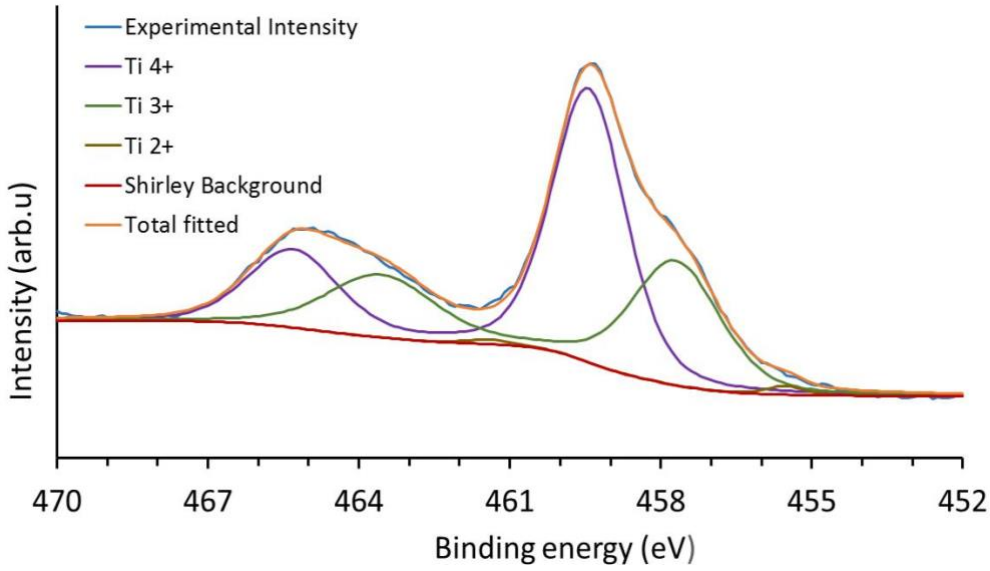

Figure 3.2: Ti XP spectra fitted with the Shirley background and showing the amount of defect sites (Ti^{3+} and Ti^{2+}). The sample was heated to 300ºC and sputtered with a dose of 2×10^{15} ions/cm^2.

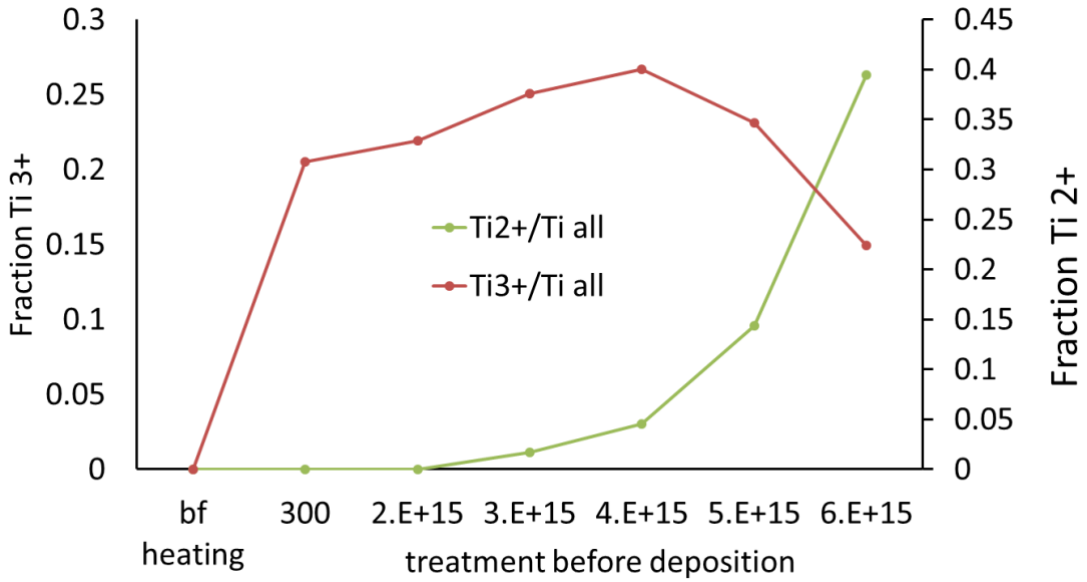

Figure 3.3: Relative number of Ti^{3+} and Ti^{2+} sites as fraction of the total Ti XPS intensity with respect to different surface treatments. The sample to the left was untreated, the second sample to the left was heated to 300 ºC and all other samples were heated to 300 ºC and subsequently sputtered with the sputter dose shown.

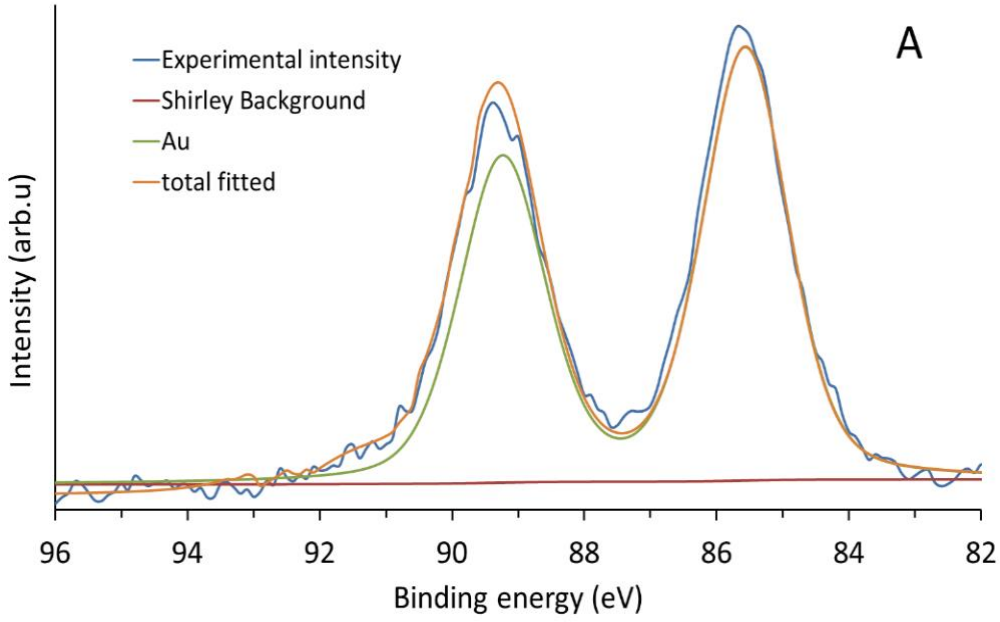

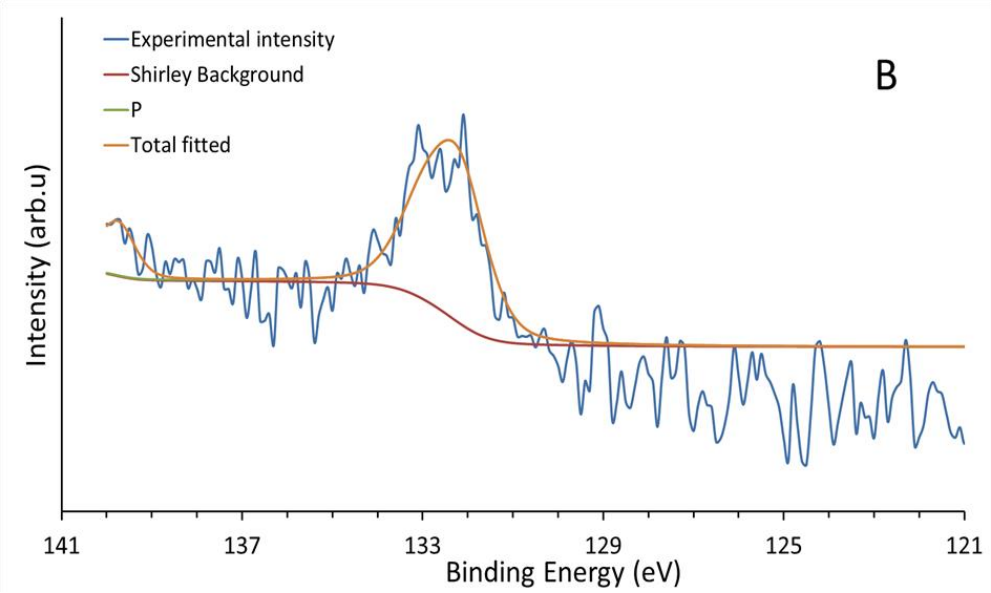

Figure 3.4: XPS peak fitting with Shirley background for (a) Au_9 (0.3 mM) after deposition and (b) P (0.3 mM) after deposition.

The peak fitting of the Au 4*f* and P 2*p* doublets, including Shirley background, are shown in figures 3.4a and 3.4b, respectively, with the fitted peak positions and FWHM presented in figure 3.5 both before and after heating. A typical XP C 1*s* spectrum after deposition and heating is shown in Figure S1 in the supporting information.

The initial and final state effect is used to distinguish the bulk Au from clusters. The initial state effect, also known as the chemical shift, defines the oxidation state of an atom, and final state effect is related to the size of the cluster and is explained in detail in our earlier papers reporting XPS of Au clusters on titania.[28-29] The final state effect causes a shift in the peak position (binding energy) and an increase in FWHM of the respective element, which is determined by the electronic structure of metal nanoclusters.[28] In case of Au_9 clusters, when the X-ray causes emission of an electron from the core level leaving a hole behind, the time taken for the outermost electron to fill the hole is greater compared to the case of the bulk Au. The peak position of the Au $4f_{7/2}$ component after deposition of Au_9 onto ALD titania is observed between 85.2 – 85.6 eV (compared to 84 eV for bulk Au). This position correlates well with findings in earlier reports which confirms the presence of intact and un-agglomerated Au_9 clusters. The FWHM of the Au $4f_{7/2}$ peaks (Figure 3.4a) is also similar to the previous measurements on Au_9 clusters.[28] The peak position of Au after heating (Figure 3.5b) shifts to lower binding energy around 84.6 – 84.8 eV, which is somewhat lower than in our earlier reports.[28, 30] At first glance, the interpretation would be that the Au clusters have slightly agglomerated. However, here the pre-treatment of the titania surface is different to previous studies and may influence the final state effect. The Au $4f_{7/2}$ peak position is the same across

all concentrations of the Au_9. Thus, the Au clusters might be in a non-agglomerated state, which is also supported by the FWHM of the Au $4f_{7/2}$ peaks after heating. Also the ratio of Au to Ti intensity ratio in XPS does not decrease due to the post-treatment of the samples, which gives further evidence that the clusters do not agglomerate due to heat treatment. If there is drop in the ratio intensity of Au to Ti, then the gold clusters tend to form the large particles which would result in the shifting of peak position towards the energy range of bulk gold (84eV). Dimer formation would add another contribution as peak at somewhat lower binding energy with the position higher in binding energy than the nanoparticles, i.e. > 84 eV. This contribution and the non-agglomerated position would then be difficult to separate in XPS but would move the centre of the Au 4f7/2 to somewhat lower binding energy. The strong hints of non-agglomeration are shown in [21,30,31] but it's hard to draw final conclusion that the clusters didn't undergo agglomeration. Surface imaging might be an alternative method to study the degree of agglomeration but it is difficult to image them after the post treatment .[34] This will be discussed further below in the context of Figure 3.6b. The MIES investigations described below also supports an interpretation of non-agglomeration and is discussed below. The reason for the lower binding energy of the Au $4f_{7/2}$ peaks after applying the post-treatment could be that the interaction of the Au with the defect rich titania causes some chemical shift to a lower binding energy of Au additional to the final state effect. It needs to be noted that initial and final state effects are difficult to separate in XPS.

O vacancies are electron rich defects which could be attractive for the positively charged [Au9 (PPh3)8]$^{3+}$ ligated core. However, other ions like those resulting from the dissociation of the solvent could also be attracted to defects and for this reason it is unclear whether the electrostatic interaction between the $[Au_9(PPh_3)_8]^+$cation and the negative charge at an O vacancy is a prevalent mechanism for the adsorption of the Au clusters.

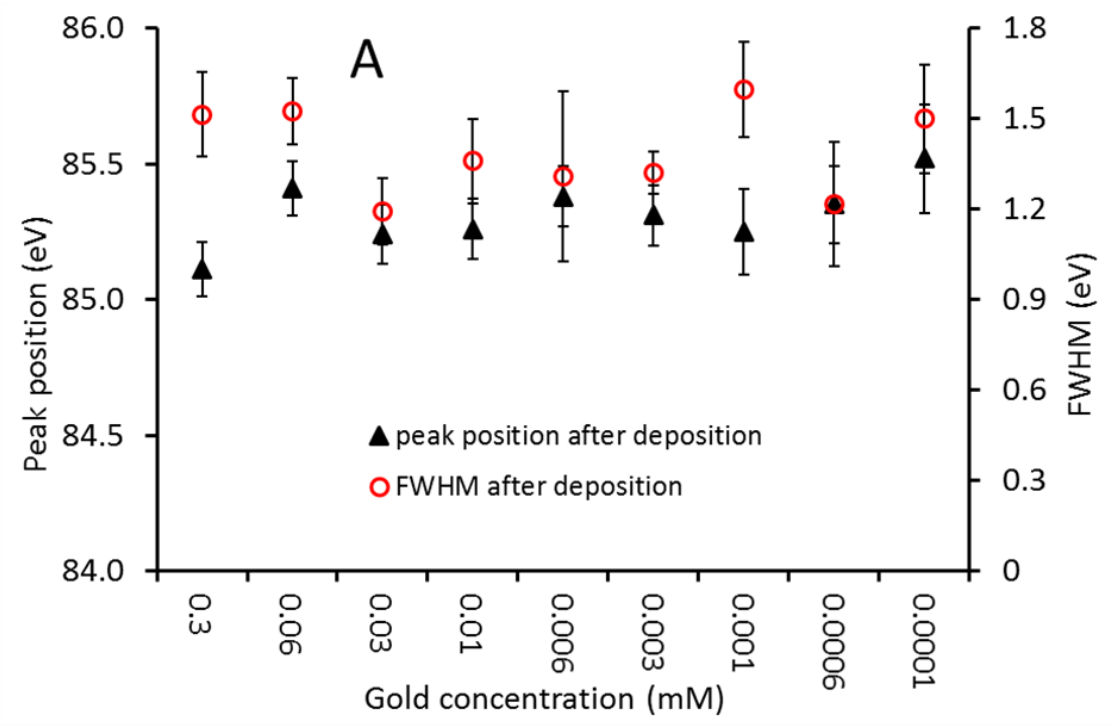
A
86.0
85.5
85.0
84.5
84.0
Peak position (eV)
1.8
1.5
1.2
0.9
0.6
0.3
0
FWHM (eV)
peak position after deposition
FWHM after deposition
0.3
0.06
0.03
0.01
0.006
0.003
0.001
0.0006
0.0001
Gold concentration (mM)

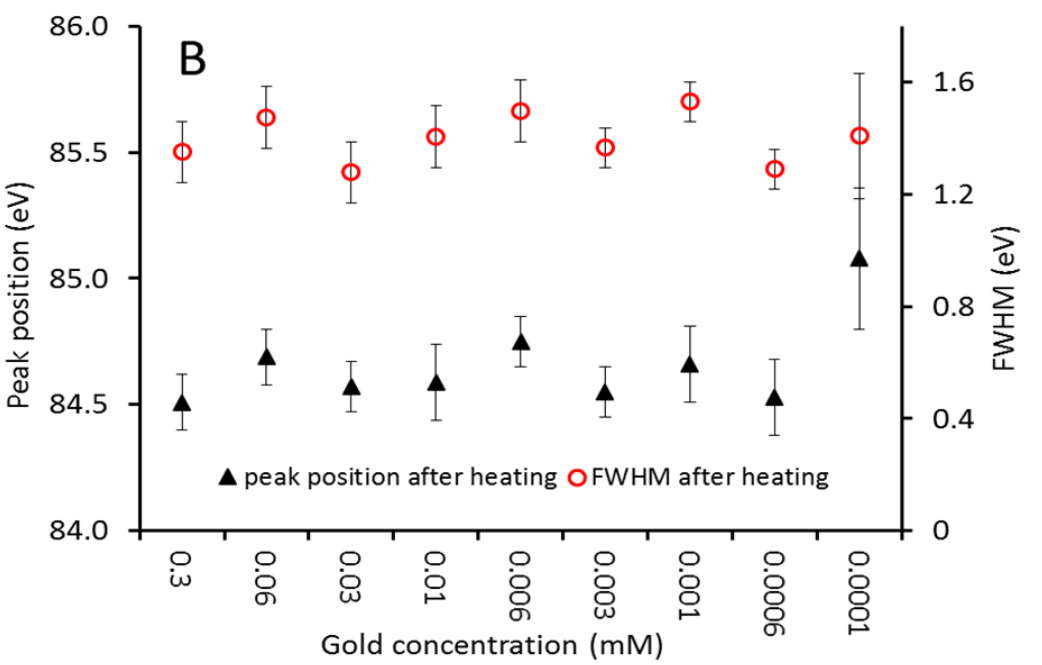
B
86.0
85.5
85.0
84.5
84.0
Peak position (eV)
1.6
1.2
0.8
0.4
0
FWHM (eV)
peak position after heating
FWHM after heating
0.3
0.06
0.03
0.01
0.006
0.003
0.001
0.0006
0.0001
Gold concentration (mM)

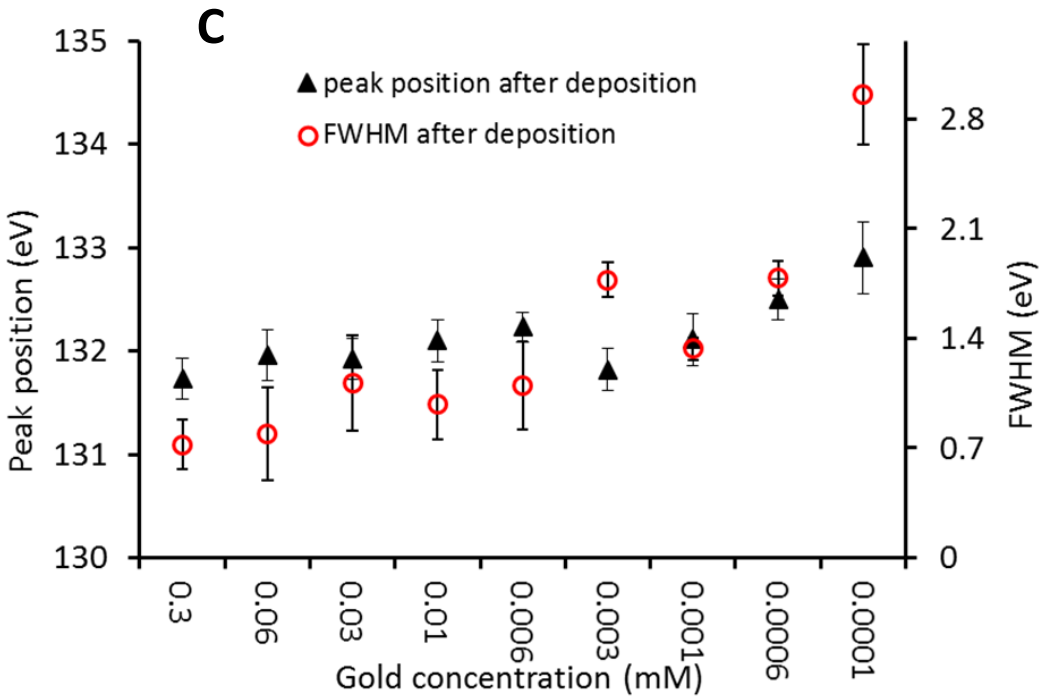
C
135
134
133
132
131
130
Peak position (eV)
2.8
2.1
1.4
0.7
0
FWHM (eV)
peak position after deposition
FWHM after deposition
0.3
0.06
0.03
0.01
0.006
0.003
0.001
0.0006
0.0001
Gold concentration (mM)

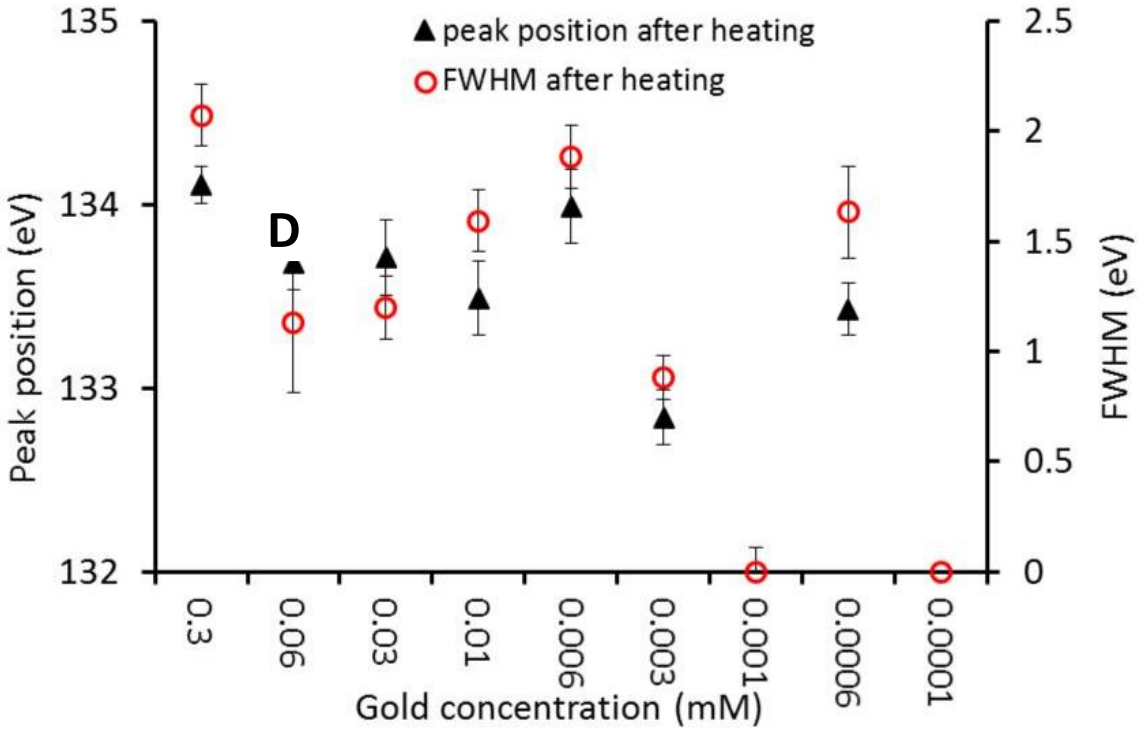

Figure 3.5: Peak position and FWHM of Au (a) after deposition and (b) after heating. Peak position and FWHM of P (c) after deposition and (d) after heating. The error bars reflect the uncertainty in the fitting procedure.

The peak positions of P after deposition of Au_9 clusters on ALD titania are found around 131.8 – 132.6 eV (Figure 3.5c). This peak position corresponds to triphenylphosphine ligands bound to Au_9 clusters as found in our previous work.[30] After heating the samples, the peak position of P shifts to higher binding energy, around 133 – 134 eV (Figure 3.5d). This binding energy corresponds to oxidized P attached to the substrate which has been observed and explained previously.[30] Note that no evidence of the $NO3^-$ counter ions is seen in XPS as also described previously.[31]

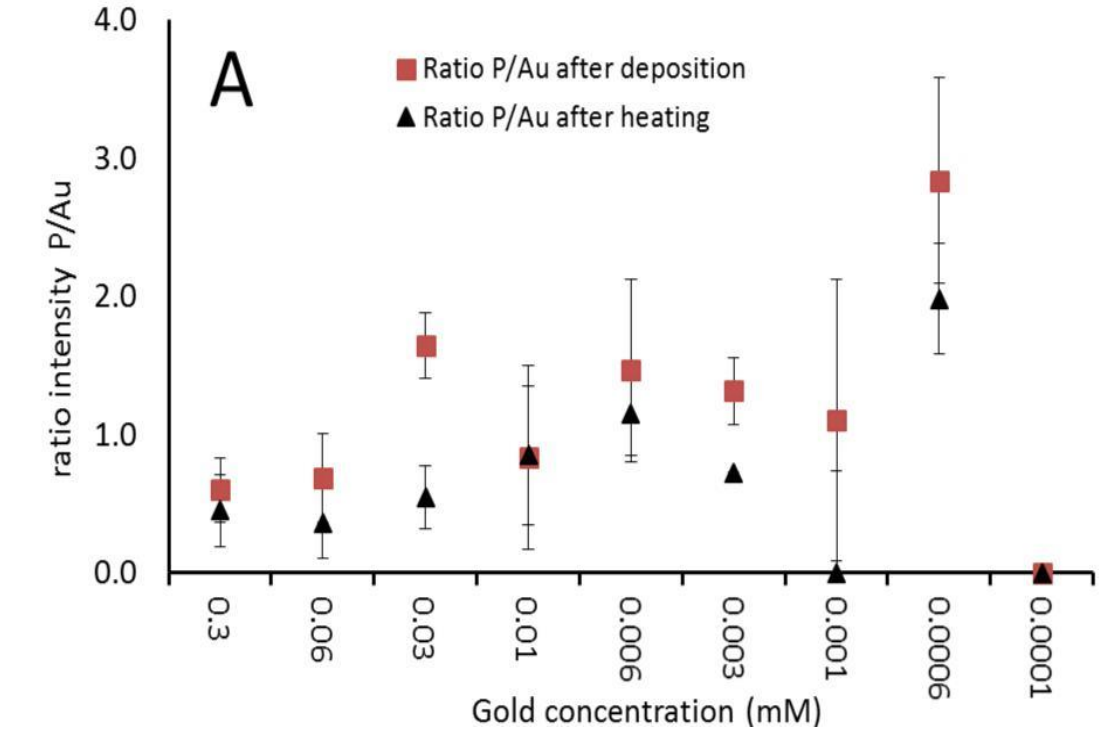
A
Ratio P/Au after deposition
Ratio P/Au after heating
ratio intensity P/Au
4.0
3.0
2.0
1.0
0.0
0.3
0.06
0.03
0.01
0.006
0.003
0.001
0.0006
0.0001
Gold concentration (mM)

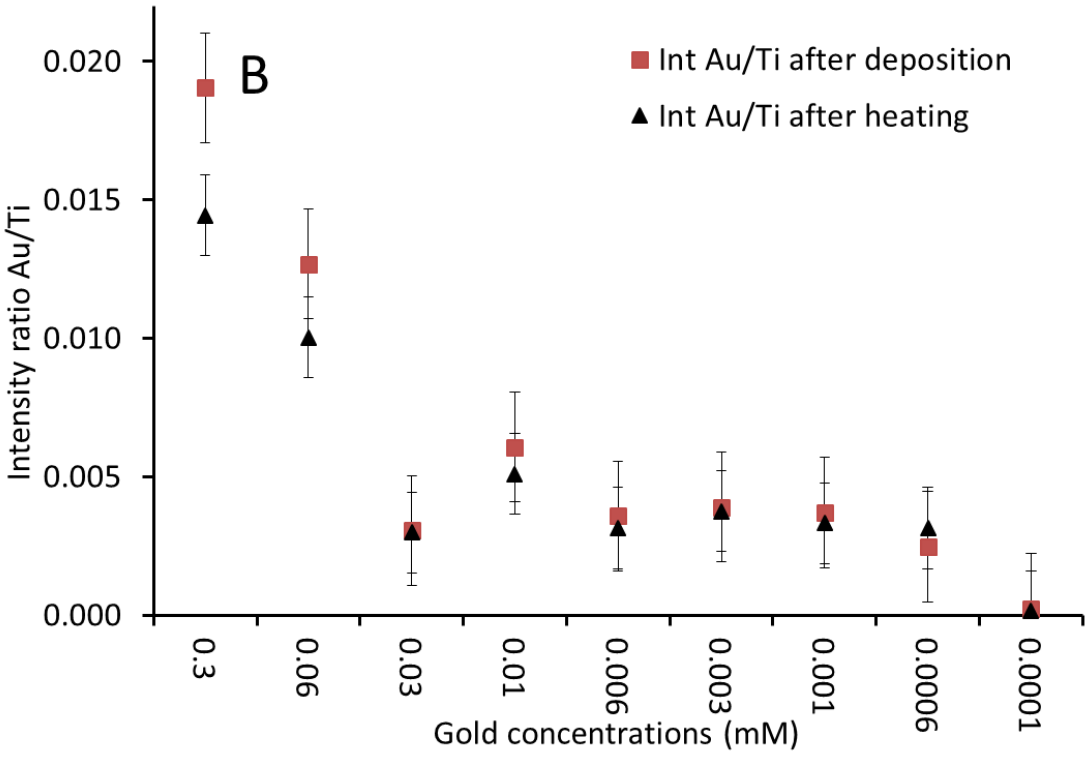
B
Int Au/Ti after deposition
Int Au/Ti after heating
Intensity ratio Au/Ti
0.020
0.015
0.010
0.005
0.000
0.3
0.06
0.03
0.01
0.006
0.003
0.001
0.0006
0.0001
Gold concentrations (mM)

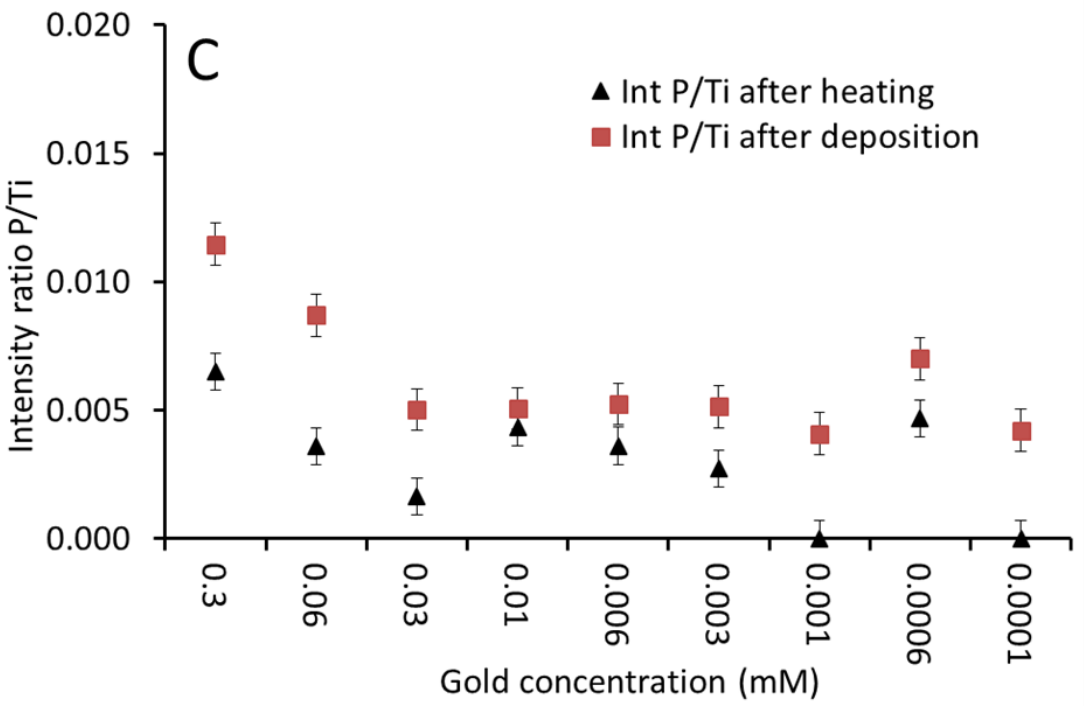

Figure 3.6: Ratio of XPS intensities after deposition of the Au_9 clusters and subsequent heating % ratio intensity of P to Au, (b) ratio of Au to Ti, and. (c) ratio of P to Ti. Note that the P/Au and P/Ti ratios are systematically lower after heating. The value of 0.01 in (b) corresponds approximately to 15% of a monolayer of Au clusters on titania as estimated by applying equation (2).

Figure 3.6a shows the ratio intensity of P to Au after deposition and post heating, which generally decreases after heating. It is estimated that approximately 50 to 80% of the ligands remain attached to the titania surface. The mechanism for the attachment of the ligands to the titania surface is described by us previously.[28]

The intensity ratio of Au to Ti shown in Figure 3.6b is almost the same after deposition and heating, resulting in the same amount of Au on the ALD titania surface. This is an indication that after heating that the clusters do not strongly agglomerate at low to medium concentrations (up to 0.03 mM). If the clusters were to agglomerate to form a nanoparticle, the Au intensity in the spectra would decrease due to the limited electron mean free path (i.e. the Au atoms at the bottom of a nanoparticle near the substrate surface would contribute less to the overall Au intensity.[30] By applying equation (2), it is estimated that the Au:Ti intensity ratio of 0.01 in Figure 3.6b corresponds approximately to 15% of a monolayer of Au clusters on titania, which is approximately one order of magnitude higher than depositing Au_9 clusters on plasma cleaned

ALD titania in our previous work.[31]Finally, Figure 3.6c shows that the ratio intensity of P to Ti decreases after heating, confirming that only a fraction of the ligands remains attached to the surface and that the rest has detached and evaporated from the sample.

3.3.2. MIES results

A series of MIES spectra of prepared samples using various Au_9 concentrations (0.3 to 0.0001 mM) and heated to 200 °C for 20 minutes are shown in Figure 3.7a. The intensity of the measured MIES spectra was normalized with the pre-treated ALD titania such that the MIES intensities of the spectra of all samples after heating and sputtering were the same within experimental uncertainty. This normalization procedure is possible because the shape of all MIE spectra of the substrates after heating and sputtering was the same within data scattering. The normalization procedure eliminates variations in the intensity of He* source.

The procedure for evaluation of the MIES spectra of the samples after applying the heat treatment after deposition of the clusters is as follows:

1) Determination of number of base spectra required to fit the measured series of MIES spectra using the SVD algorithm.
2) Determination of the meaningful reference spectra.
3) Interpretation of the nature of reference spectra.

1. Determination of the number of base spectra required using SVD algorithm:

Our application of the SVD algorithm has been explained in detail previously [20] so herein we only summarize the main aspects of the procedure. The first step determines the number of base spectra required to fit the entire series of measured MIES spectra shown in Figure 3.7a. As a result of the SVD algorithm, the number of base spectra required for fitting the series of MIES spectra is two.

2. Determination of meaningful reference spectra:

In the second step the number of reference spectra are determined and in this case it is the same as the number of base spectra i.e. two reference spectra. The two main assumptions in the procedure for determining the reference spectra are (i) that the reference spectra should be non-negative and (ii) that the sum of the weighting factors should be close to unity which results in the meaningful reference spectra. The procedure used here and by us previously[31] differs in the second step from the procedure described by Berlich *et al.*[32]

The second reference spectra is defined by following the procedure outlined by Andersson *etal.*[31]. The reproducibility of the reference spectra is discussed in the supporting information

in the context of Figures 3.3 and S3. The reference spectra are shown in Figure 3.7b using two energy scales. The kinetic energy scale (bottom axis) holds for both reference spectra while the binding energy scale (top axis) holds only for reference spectrum 2. The reason is that the de-excitation mechanisms leading to the emission of electrons upon excitation with He* are different. Titania has states close to the Fermi edge as can be seen in the UP spectra in Figure 3.7d. He* are de-excited via resonant ionization and Auger neutralization which leads to a self-convolution and blurring of the features in the spectra. The de-excitation of He* interacting with the Au clusters is considered as Auger de-excitation because the Au clusters can be considered as small molecules. In the Auger de-excitation mechanism there is a direct correlation between binding energy of the emitted electron before its excitation and the kinetic energy of the emitted electron and equation 3 applies. For resonant ionization and Auger neutralization no simple relationship exists and thus the relationship between binding energy and kinetic energy cannot be expressed in an equation equivalent to equation 3.

3. Interpretation of reference spectra:

The pre-treated blank ALD titania sample heated to 200 °C for 20 minutes was found to be one of the reference spectra. The weighting factor α is shown in Figure 3.7c. The nature of the second reference spectra is identified by comparing the weighting factors obtained from SVD with the relative intensity of the elements in the XPS analysis. The plot of weighting factors from SVD compared against the XPS relative intensity of Au to Ti and P to Ti is also shown in Figure 3.7c. The weighting factors from MIES for the reference spectrum 2 (defined as β) follows the same pattern as a combination of the relative intensity of Au and P with respect to titania irrespective of the scattering. Thus, the second reference spectra from MIES spectra is associated with the presence of the Au clusters and P ligands detached from the clusters. Modification of titania due to the presence of the clusters and the ligands could also contribute to the second reference spectrum. The second reference spectrum from the MIE spectrum starts between 1 and 2 eV (binding energy scale) as can be seen in the inset in Figure 3.7b. The position of 3.4 ± 0.1 eV (vertical blue line in the inset) coincides with the position of the valence band cut-off found through UPS (Figure 3.7d, also see Figure S7 in the supporting information and associated text). Since the MIES binding energy scale has the same binding energy scale as that of the UP spectra (*vide supra*), it is clear that there are spectral contributions from the Au_9 clusters below the TiO_2 valence band. The second reference spectrum also has prominent features at binding energies 4.4, 7.3 and 9.4 eV. The positions of these features can be compared with the reference spectra shown in our previous work,[31] which identified three reference spectra attributed to (i) titania, (ii) the presence of Au_9 clusters on O plasma treated ALD titania, and (iii) phosphine ligands. In that work ,[31] the reference

spectrum attributed to the DOS of Au_9 clusters at binding energy 4 – 6 eV and 7 – 9 eV, and the reference spectrum attributed to the presence of triphenylphosphine ligands has states at binding energy between 10 – 12 eV. The reference spectrum 2 of the present work is thus a combination of the reference spectra attributed to Au_9 and the triphenylphosphine ligands in the previous work. In case the weighting for two of the reference spectra have a constant ratio across a series of measurements, the SVD algorithm is not able to separate these two reference spectra. We assume this is just a coincidence in the present set of data. The interpretation of the re-measured samples results in the same features except the features from the secondary electron contribution, which is shown in supporting information (see Figure S4). The reference spectrum related to the Au clusters in our previous work [31]does not identify any intensity at a binding energy less than 4 eV. The reason is that the S/N ratio is higher in the present work because the density of the Au clusters on the titania surface is higher (*vide supra*). An estimate for the coverage of the titania surface with Au_9 clusters is ~15% monolayer at an intensity ratio of 0.01 in Figure 3.6c. It is important to emphasize that the surface treatment before deposition of the clusters was different in the previous work.[31]

In Figure 3.7d the low binding energy region of the UP spectrum is shown together with the IPE spectrum after the pre-treatment, including the extrapolations for determining the valence band and conduction band cut-offs for titania. The feature near the energy range 1eV represents the Ti^{3+} species (oxygen vacancy site).[31]

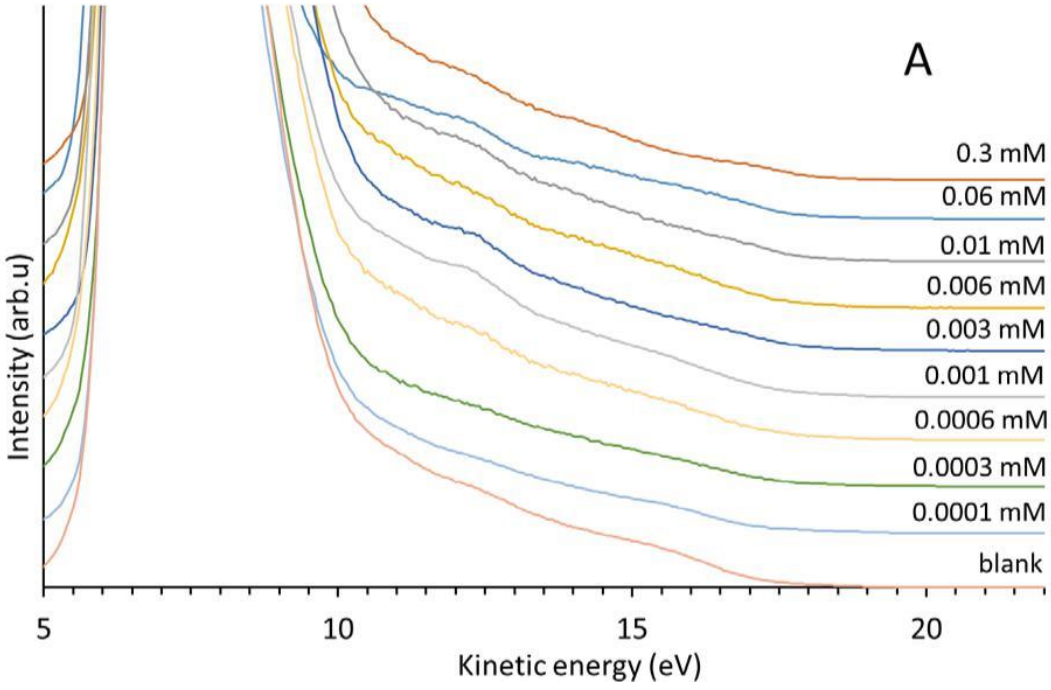

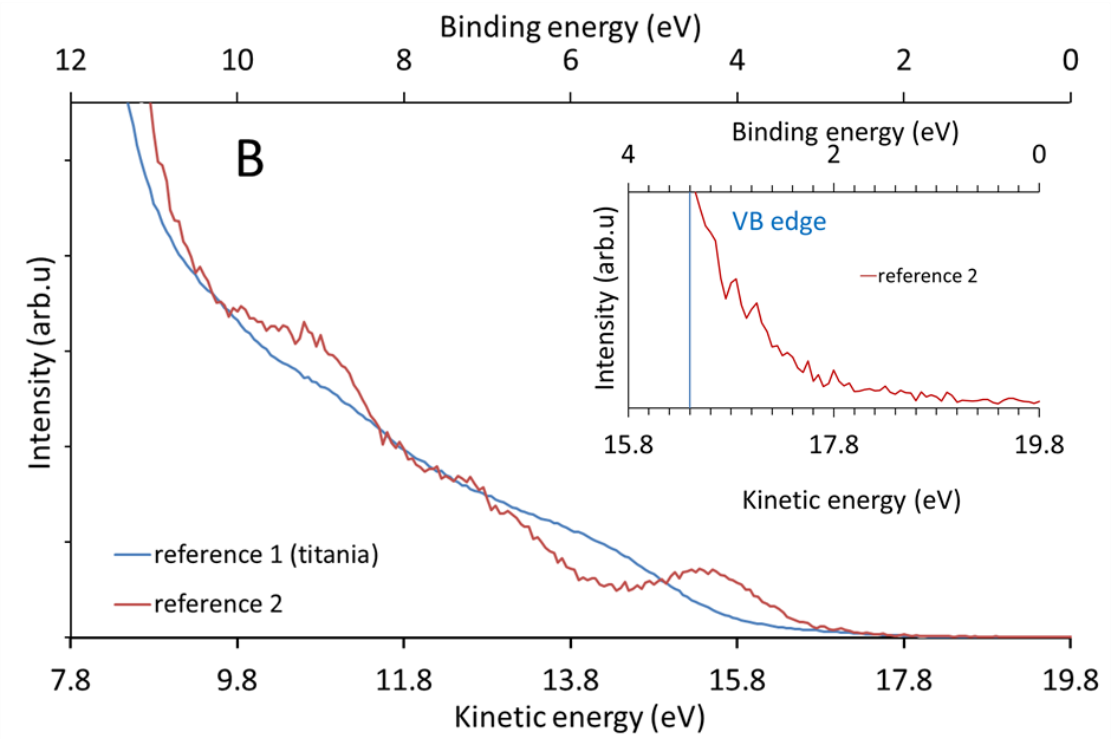
Binding energy (eV)
12
10
8
6
4
2
0
B
Intensity (arb.u)
Binding energy (eV)
4
2
0
VB edge
reference 2
Intensity (arb.u)
15.8
17.8
19.8
Kinetic energy (eV)
reference 1 (titania)
reference 2
7.8
9.8
11.8
13.8
15.8
17.8
19.8
Kinetic energy (eV)

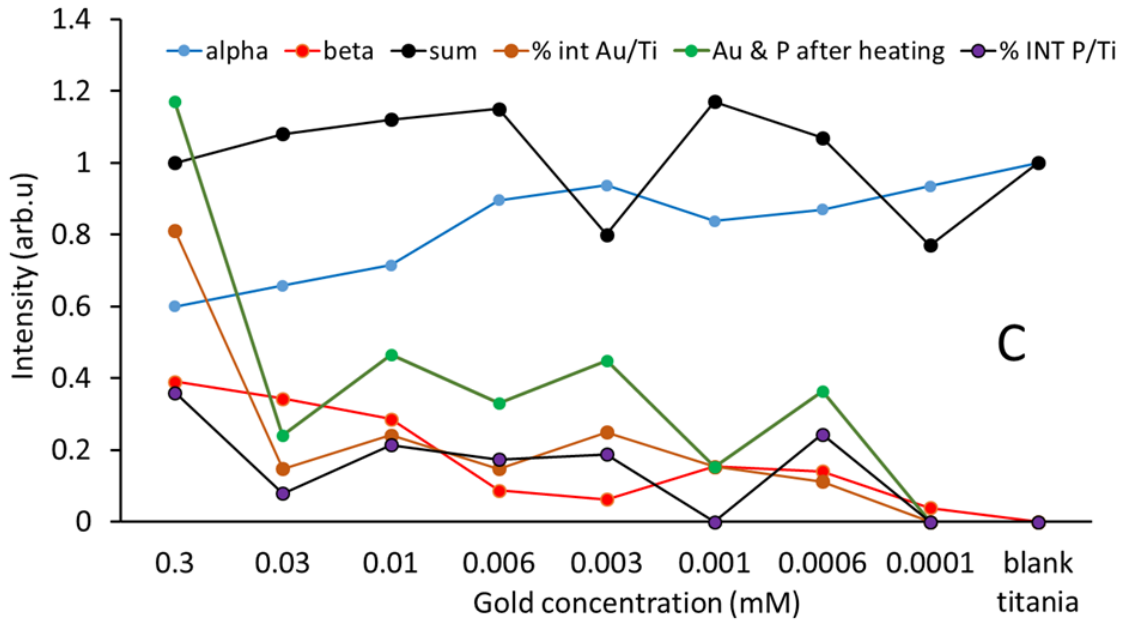
alpha
beta
sum
% int Au/Ti
Au & P after heating
% INT P/Ti
Intensity (arb.u)
1.4
1.2
1
0.8
0.6
0.4
0.2
0
C
0.3
0.03
0.01
0.006
0.003
0.001
0.0006
0.0001
blank titania
Gold concentration (mM)

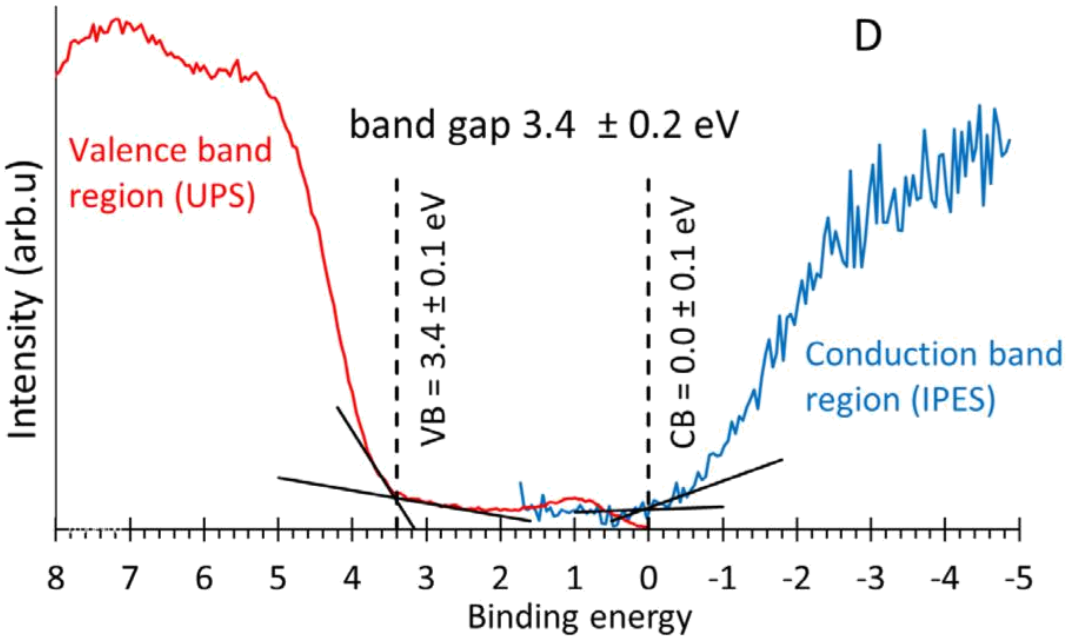

Figure 3.7: (a) MIES spectra of various Au concentrations after heating (b) MIES reference spectra after heating; reference spectrum 1 is identified as the heated and sputtered substrate and reference spectrum 2 is due to the presence of the Au clusters after ligand detachment from the cluster core with the region 0 to 4 eV in binding energy shown in the inset. The lower horizontal scale is in kinetic energy of the electrons and holds for both reference spectra while the upper scale is the binding energy and holds only for reference spectrum 2 (see further explanation in the main body). (c) Plots of weighting factors α and β from MIES as well as their sum, XPS intensity of Au and P normalized to the Ti intensity, and the sum of the Au and P intensity against gold concentration. In (d) the UP and IPE spectrum in the region around the band gap after the pre-treatment are shown with the position of the valence band and conduction band cut-offs (VB and CB respectively).

Computer Calculations

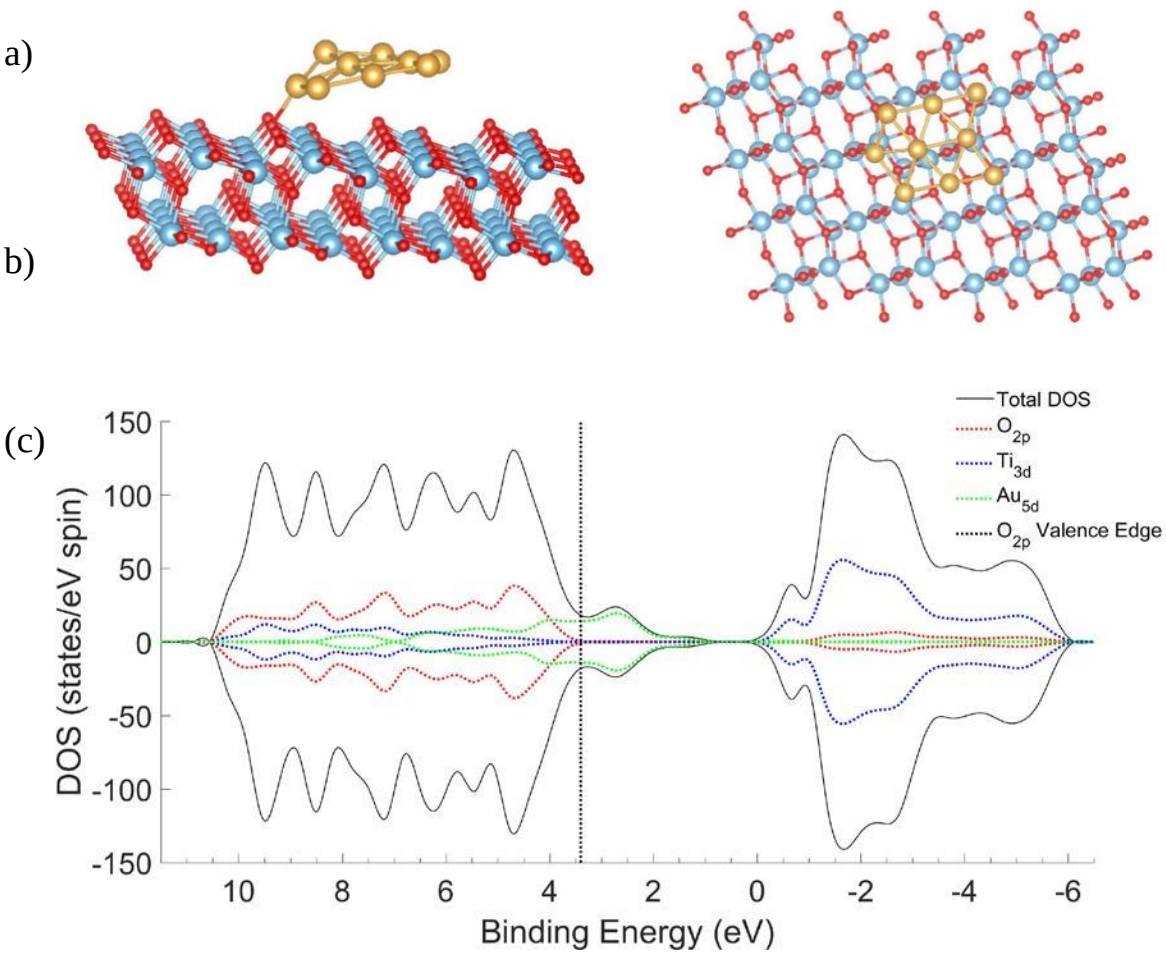

Figure 3.8: Relaxed structure of Au_9/TiO_2 from side view (a) and top view (b) calculated by DFT. In (c) the LPDOS of surface O 2p, Ti 3d, Au 5d are shown, as well as the total DOS (i.e. bulk structure). For comparison with the experiment the energies are scaled and calibrated to the O 2p valence edge (denoted by the dotted vertical line) and Ti 3d conduction edge. Furthers detail about the scaling is given in the main body of the manuscript.

A recent DFT calculation identified the lowest energy structure of a Au_9 cluster attached onto a TiO_2 (001) surface to be 2D and essentially planar,[33] consistent with results from our previous STEM study of Au_9 on titania nanosheets.[34] Starting with a planar Au_9 cluster geometry, our DFT optimized structure of Au_9 on an anatase (101) surface is similar, as shown in Figure 3.8 (a) and (b) A slight bending of the planar Au_9 cluster is evident after the geometry optimization, and results in Au_9 cluster adsorption energy of −0.37 eV. The average bond lengths were found to be 2.71 Å for Au-Au and 2.28 Å for Au-O_{2c} bonds, respectively. These bond lengths are similar to the literature reported Au_9/TiO_2 (001) lowest energy structure, however, we do not observe any surface reconstruction with the (101) surface as found for the (001) surface.

To examine the electronic structure of the relaxed geometry in detail, the localized projected densities of states (LPDOS) was calculated for Au_9/TiO_2 and is shown in Figure S8 in the supporting information. The electronic energy of the highest occupied O 2*p* state (*i.e.* valence edge) is –4.44 eV (dotted vertical line) and the lowest energy Ti 3*d* unoccupied state (*i.e.* conduction edge) is at –1.92 eV, which we define as the TiO_2 "band gap" with a calculated value of 2.52 eV. The onset of Au_9 density is at –2.83 eV, approximately 1.6 eV below the valence edge, and prominent features are observed at –3.9 eV and –5.1 eV, around 0.5 eV below and 0.7 eV above the TiO_2 valence edge, respectively. Therefore, it is clear that the Au_9 cluster has introduced states within the TiO_2 band gap.

Comparison between measured and calculated DOS

When comparing calculated energy levels to experiments, it is necessary to firstly consider the energies relative to a common point,[35] in this case the TiO_2 valence and conduction edges.[35] (Note that in calculations, increasing binding energies correlate with a decreasing scale of negative value, whereas experimental data conventionally shows increasing binding energies on an increasing scale with positive values.) A linear scale of the calculated DOS eigenvalues was employed to expand the calculated TiO_2 "band gap" to the value measured by UPS and IPES in Figure 3.7d (*i.e.* 3.4 eV). The O 2*p* valence edge was then shifted to +3.4 eV (as determined from UPS). The resultant LPDOS plot is shown in Figure 3.8(c) having a binding energy scale that allows direct comparison with the MIE spectrum of Figure 3.7 (b).

The onset of reference spectrum 2 in Figure 3.6(b) appears at a binding energy of around 1.8 eV and is assigned to the adsorption of Au_9 clusters onto the ALD titania surface. The DFT calculated states assigned to the presence of Au_9 clusters on the TiO_2 (101) surface emerge at ~1.2 eV binding energy, increasing significantly at 1.8 eV. Therefore, the position of the DOS of the Au_9 clusters found in MIES and in the DFT calculation are comparable. It should be noted that the exact shape and intensity of the DOS determined with DFT and electron spectroscopy must be different due the nature of the applied experimental methods. One example is that the shape of the electron spectra is strongly influenced by the transmission function of the analyser and the cross section for the interaction of He* with the electron density in the sample. For this reason only semi-quantitative comparison between DFT and electron spectroscopy experiments can be made.

It should be noted that the titania surface used for the theoretical calculation is the anatase (101) planar surface which is different to that of the experimental study where the titania surface employed here polycrystalline anatase which has defects introduced but this was the best we could achieve at that moment.

3.4. Conclusion

Chemically synthesized atomically precise phosphine stabilized Au_9 clusters deposited onto the pre-treated ALD titania after heating to 200 ºC for 20 minutes was investigated using XPS and MIES. XPS results revealed that the Au_9 clusters deposited on the pre-treated ALD titania are most likely not agglomerated after the post heat treatment but found at a binding energy slightly lower than observed previously. The triphenylphosphine ligands are completely removed from the Au_9 surface and found oxidized onto the ALD titania surface. The MIES results revealed that two reference spectra are required to explain the electronic structure of the sample. One reference spectrum is related to the titania substrate while the second spectrum is related to the presence of the Au clusters and the ligands removed from the cluster cores.

An important outcome of the present work is that defects introduced into the ALD titania surface via sputtering and heating strongly reduces the agglomeration of the Au clusters adsorbed to the surface. In our previous work ligand stabilized showed a significant degree of agglomeration when deposited onto defect poor ALD titania surfaces.[31]

The interpretation of the reference spectrum of the Au clusters shows that the Au states which can be clearly identified in the MIE spectra have their lowest binding energy at approximately 1.8 eV. The observed DOS of Au_9 are comparable to those calculated by DFT.

Supporting Information:

Details fitting of XP spectra, details XPS regarding generation of vacancies, reproducibility of MIE spectra, UP spectra, results DFT calculation.

3.5. References

1. Borman, V. D.; Pushkin, M. A.; Tronin, V. N.; Troyan, V. I., Evolution of the Electronic Properties of Transition Metal Nanoclusters on Graphite Surface. *Journal ofExperimental and Theoretical Physics* **2010**, *110*, 1005-1025.

2. Kitsudo, Y.; Iwamoto, A.; Matsumoto, H.; Mitsuhara, K.; Nishimura, T.; Takizawa, M.; Akita, T.; Maeda, Y.; Kido, Y., Final State Effect for Au 4f Line from Gold-Nano-Particles Grown on Oxides and Hopg Supports. *Surface Science***2009**, *603*, 2108-2114.

3. Chusuei, C. C.; Lai, X.; Davis, K. A.; Bowers, E. K.; Fackler, J. P.; Goodman, D. W., A Nanoscale Model Catalyst Preparation: Solution Deposition of Phosphine-Stabilized Gold Clusters onto a Planar Tio2 (110) Support. *Langmuir***2001**, *17*, 4113-4117.

4. Ahmad, M. Z.; Sadek, A. Z.; Yaacob, M. H.; Anderson, D. P.; Matthews, G.; Golovko, V. B.; Wlodarski, W., Optical Characterisation of Nanostructured Au/Wo3 Thin Films for Sensing Hydrogen at Low Concentrations. *Sensors and Actuators B: Chemical***2013**, *179*, 125-130.

5. Ahmad, M. Z.; Golovko, V. B.; Adnan, R. H.; Abu Bakar, F.; Ruzicka, J.-Y.; Anderson, D. P.; Andersson, G. G.; Wlodarski, W., Hydrogen Sensing Using Gold Nanoclusters Supported on Tungsten Trioxide Thin Films. *International Journal of Hydrogen Energy***2013**, *38*, 12865-12877.

6. Clavero, C., Plasmon-Induced Hot-Electron Generation at Nanoparticle/Metal-Oxide Interfaces for Photovoltaic and Photocatalytic Devices. *Nat Photon***2014**, *8*, 95-103.

7. Chen, Y.-S.; Choi, H.; Kamat, P. V., Metal-Cluster-Sensitized Solar Cells. A New Class of Thiolated Gold Sensitizers Delivering Efficiency Greater Than 2%. *J. Am. Chem. Soc.***2013**, *135*, 8822-8825.

8. Wood, V.; Panzer, M. J.; Halpert, J. E.; Caruge, J. M.; Bawendi, M. G.; Bulović, V., Selection of Metal Oxide Charge Transport Layers for Colloidal Quantum Dot Leds. *ACS Nano***2009**,*3*, 3581-3586.

9. Chen, M.; Goodman, D. W., Catalytically Active Gold on Ordered Titania Supports. *Chem. Soc. Rev.* **2008**, *37*, 1860-1870.

10. Choudhary, T. V.; Goodman, D. W., Catalytically Active Gold: The Role of Cluster Morphology. *Applied Catalysis A: General* **2005**, *291*, 32-36.

11. Turner, M.; Golovko, V. B.; Vaughan, O. P. H.; Abdulkin, P.; Berenguer-Murcia, A.; Tikhov, M. S.; Johnson, B. F. G.; Lambert, R. M., Selective Oxidation with Dioxygen by Gold Nanoparticle Catalysts Derived from 55-Atom Clusters. *Nature***2008**, *454*, 981-983.

12. Min, B. K.; Wallace, W. T.; Goodman, D. W., Support Effects on the Nucleation, Growth, and Morphology of Gold Nano-Clusters. *Surface Science***2006**, *600*, L7-L11.

13. Bagheri, S.; Muhd Julkapli, N.; Bee Abd Hamid, S., Titanium Dioxide as a Catalyst Support in Heterogeneous Catalysis. *The Scientific World Journal***2014**, *2014*, 21.

14. Li, G.; Jin, R., Atomically Precise Gold Nanoclusters as New Model Catalysts. *Accounts of Chemical Research* **2013**, *46*, 1749-1758.

15. Liu, Y.; Tsunoyama, H.; Akita, T.; Xie, S.; Tsukuda, T., Aerobic Oxidation of Cyclohexane Catalyzed by Size-Controlled Au Clusters on Hydroxyapatite: Size Effect in the Sub-2 Nm Regime. *ACS Catalysis***2011**, *1*, 2-6.

16. Heiz, U.; Bullock, E. L., Fundamental Aspects of Catalysis on Supported Metal Clusters. *Journal of Materials Chemistry***2004**, *14*, 564-577.

17. Valden, M.; Lai, X.; Goodman, D. W., Onset of Catalytic Activity of Gold Clusters on Titania with the Appearance of Nonmetallic Properties. *Science***1998**, *281*, 1647-1650.

18. Bennett, T.; Adnan, R. H.; Alvino, J. F.; Kler, R.; Golovko, V. B.; Metha, G. F.; Andersson, G. G., Effect of Gold Nanoclusters on the Production of Ti3+ Defect Sites in Titanium Dioxide Nanoparticles under Ultraviolet and Soft X-Ray Radiation. *The Journal of Physical Chemistry C* **2015**, *119*, 11171-11177.

19. Wang, Y., et al., Role of Point Defects on the Reactivity of Reconstructed Anatase Titanium Dioxide (001) Surface. *Nat Commun***2013**, *4*, 2214.

20. Bennett, T.; Adnan, R. H.; Alvino, J. F.; Golovko, V.; Andersson, G. G.; Metha, G. F., Identification of the Vibrational Modes in the Far-Infrared Spectra of Ruthenium Carbonyl Clusters and the Effect of Gold Substitution. *Inorg. Chem.***2014**, *53*, 4340-4349.

21. Al Qahtani, H. S.; Metha, G. F.; Walsh, R. B.; Golovko, V. B.; Andersson, G. G.; Nakayama, T., Aggregation Behavior of Ligand-Protected Au9 Clusters on Sputtered Atomic Layer Deposition Tio2. *The Journal of Physical Chemistry C***2017**, *121*, 10781-10789.

22. Xiong, L.-B.; Li, J.-L.; Yang, B.; Yu, Y., Ti3+in the Surface of Titanium Dioxide: Generation, Properties and Photocatalytic Application. *J. Nanomat.***2012**, *2012*, 13.

23. Wallace, W. T.; Min, B. K.; Goodman, D. W., The Stabilization of Supported Gold Clusters by Surface Defects. *Journal of Molecular Catalysis A: Chemical***2005**, *228*, 3-10.

24. Hungria, A. B.; Raja, R.; Adams, R. D.; Captain, B.; Thomas, J. M.; Midgley, P. A.; Golovko, V.; Johnson, B. F. G., Single-Step Conversion of Dimethyl Terephthalate into

Cyclohexanedimethanol with Ru5ptsn, a Trimetallic Nanoparticle Catalyst. *Angew. Chem. Int. Ed.* **2006**, *45*, 4782-4785.

25. Raja, R.; Golovko, V. B.; Thomas, J. M.; Berenguer-Murcia, A.; Zhou, W.; Xie, S.; Johnson, B. F. G., Highly Efficient Catalysts for the Hydrogenation of Nitro-Substituted Aromatics. *Chemical Communications***2005**, 2026-2028.

26. Shirley, D. A., High-Resolution X-Ray Photoemission Spectrum of the Valence Bands of Gold. *Phys. Rev. B***1972**, *5*, 4709-4714.

27. Wahlstrom, E.; Lopez, N.; Schaub, R.; Thostrup, P.; Ronnau, A.; Africh, C.; Laegsgaard, E.; Norskov, J. K.; Besenbacher, F., Bonding of Gold Nanoclusters to Oxygen Vacancies on Rutile Tio2(110). *Phys Rev Lett***2003**, *90*, 026101.

28. Anderson, D. P.; Alvino, J. F.; Gentleman, A.; Qahtani, H. A.; Thomsen, L.; Polson, M. I.; Metha, G. F.; Golovko, V. B.; Andersson, G. G., Chemically-Synthesised, Atomically-Precise Gold Clusters Deposited and Activated on Titania. *Phys Chem Chem Phys***2013**, *15*, 3917-29.

29. Ruzicka, J.-Y.; Abu Bakar, F.; Hoeck, C.; Adnan, R.; McNicoll, C.; Kemmitt, T.; Cowie, B. C.; Metha, G. F.; Andersson, G. G.; Golovko, V. B., Toward Control of Gold Cluster Aggregation on Tio2 Via Surface Treatments. *The Journal of Physical Chemistry C***2015**, *119*, 24465-24474.

30. Anderson, D. P., et al., Chemically-Synthesised, Atomically-Precise Gold Clusters Deposited and Activated on Titania. Part Ii. *Phys. Chem. Chem. Phys.***2013**, *15*, 14806-13.

31. Andersson, G. G., et al., Phosphine-Stabilised Au9 Clusters Interacting with Titania and Silica Surfaces: The First Evidence for the Density of States Signature of the Support-Immobilised Cluster. *J. Chem. Phys.***2014**, *141*, 014702.

32. Berlich, A.; Liu, Y. C.; Morgner, H., Evaporation of Ni and Carbon Containing Species onto Nio/Ni as Case Study for Metal Support Catalysts Investigated by Metastable Induced Electron Spectroscopy (Mies). *Radiation Physics and Chemistry***2005**, *74*, 201-209.

33. Jiang, Z.-Y.; Zhao, Z.-Y., Density Functional Theory Study on the Metal-Support Interaction between a Au9 Cluster and an Anatase Tio2(001) Surface. *PCCP***2017**, *19*, 22069-22077.

34. Al Qahtani, H. S.; Kimoto, K.; Bennett, T.; Alvino, J. F.; Andersson, G. G.; Metha, G. F.; Golovko, V. B.; Sasaki, T.; Nakayama, T., Atomically Resolved Structure of Ligand-Protected Au9 Clusters on Tio2 Nanosheets Using Aberration-Corrected Stem. *J. Chem. Phys.***2016**,*144*, 114703.

35. Heinz, B.; Morgner, H., A Metastable Induced Electron Spectroscopy Study of Graphite: The K-Vector Dependence of the Ionization Probability. *Surf Sci.***1998**, *405*, 104-111.

Chapter 4

Investigation of Phosphine ligand protected Gold cluster [Au_{13} $(PPh_3)_8(NO_3)_3$] on defect rich ALD titania using Electron spectroscopies

This chapter is a reformatted version of the manuscript planned to be submitted to **The Journal of Physical Chemistry Letters**.

4.1. Abstract

Atomically precise chemically synthesized gold clusters protected by triphenylphosphine ligands [Au_{13} $(PPh_3)_8$ $(NO_3)_3$] were deposited onto the pre-treated atomic layer deposited titania surface. The ALD titania was heated and subsequently sputtered under ultra-high vacuum (UHV) condition for inducing defects in the titania. The gold clusters deposited onto the pre-treated titania were post heated at 200ºC for 20 minutes under UHV to remove the ligands protecting the gold clusters. The change in the electronic structure and the chemical composition after deposition and post heat treatment was investigated using metastable induced electron spectroscopy (MIES) and X-ray photoelectron spectroscopy (XPS). The MIES spectra allow identifying the density of states (DOS) of the Au_{13} clusters on the titania. The DOS of the Au_{13} are found similar compared to the previously investigated Au_9 clusters on sputtered ALD titania but shifted relative to each other in their binding energy of 0.1eV.

4.2. Introduction

Bulk gold and large gold particles usually are non-reactive. In contrast, gold clusters have been found to be catalytically active.[1-2] Gold clusters (or clusters) consist of up to 100 gold atoms and are less than 2 nanometres in size. Gold clusters supported by the metal oxide support gained attention recently in the field of photo catalysis.[3-4] The properties of gold clusters are distinctively different to the bulk gold and makes the clusters unique for photocatalytic applications. The catalytic activity of the gold clusters is associated with its electronic properties (or density of states).[5-6] Therefore, understanding and determining the electronic structure of the gold clusters on the surface as well as modification of the support surface due to the attachment of the gold clusters is crucial for understanding the photo catalysis based on Au clusters. It can be expected that the change of the electronic structure of the support surface upon attachment of the gold clusters depends on the number of atoms forming the gold cluster because the electronic structure of the gold clusters depends on the size of the cluster.[7-8] Thus, the understanding of the electronic properties and DOS of the gold clusters on semiconductor surfaces will facilitate the understanding of photocatalytic reactions. The gold clusters synthesis follows two approaches: chemical synthesis and gas phase approach. Both the approaches have advantages and disadvantages. In the chemically synthesised ligand protected clusters offers the advantage of the controllable size and coverage on the non-planar surfaces. The disadvantages include is that the ligands attached acts as the further chemical species which makes the surface complex. The ligands are then removed by heat treatment to make contact after the solution-based deposition of gold clusters with the surface of the titania. In gas-phase cluster deposition is a clean system in which the size is controlled by a mass-spectrometer to allow precise control over cluster size without the need for protecting ligands. The disadvantage is that it can be coated on non-planar surfaces. The strong interaction of the clusters with the metal oxide support helps to avoid the aggregation of the clusters. Thus, the pre-treatment of the metal oxide support serves as the suitable site for the attachment of the clusters onto the surface. The pre-treatment like heating and sputtering has shown to reduce the degree of agglomeration of clusters.[9] Titania is used here as support material because it is the widely used metal oxide support material for heterogeneous catalysis.

The aim of this work is to investigate the DOS of the surface after deposition of chemically synthesized gold clusters protected by triphenylphosphine ligands $[Au_{13}(PPh_3)_8]$ $(NO_3)_3]$ onto the pre-treated (*via* heating and sputtering) ALD TiO_2 films. The combination of the surface analytical techniques Metastable Induced Electron Spectroscopy (MIES) and Ultraviolet Photoelectron Spectroscopy (UPS) is used to study the electronic structure of the surface after

post heat treatment while X-ray Photoelectron Spectroscopy (XPS) is used to identify chemical composition of the sample surface and to observe the ligands removal after deposition and post heat treatment. The DOS of Au_{13} as determined here will be compared with the earlier measured DOS of Au_9.

4.3. Results and Discussion

4.3.1. XPS Results

XP spectra were taken for main peak elements like gold (Au 4f), phosphorous (P 2p), titania (Ti 2p), carbon (C 1s), silicon (Si 2p) and oxygen (O 1s).The Shirley background was used for fitting the peaks which removes the background electron scattering thus giving the elemental peak shape[10]. The main carbon peak (285eV) is used as the calibration peak to correct the peak position of the other elements. The carbon source emerges from the triphenylphosphine ligands and the hydrocarbons which is identified in all the samples exposed to atmospheric air corresponding to the C-C bonds. The XPS measurements were performed for a series of samples varying the gold concentration from 0.06mM to 0.0001mM The XPS measurements were performed for a series of samples varying the gold concentration from 0.06mM to 0.0001mM. The 0.03mM, 0.003mM and 0.0003mM samples showed a high degree of agglomeration in the examination of the XPS results. The reason for the agglomeration is unknown and these 3 samples were removed from the data set and not considered for further data analysis.

Surface Pre-treatment

The surface of the ALD titania was pre-treated by heating to a specific temperature to remove the hydrocarbons present on the surface followed by the sputtering technique to introduce oxygen vacancies. The temperature chosen for the pre heat treatment was 300°C and is explained in detail in.[9] The introduction of oxygen vacancies (sputtering) by bombarding the Ar^+ ions onto the surface of the ALD titania serves as suitable method for the attachment of clusters onto the surface.[3] As a result of sputtering, defect sites Ti^{3+} and Ti^{2+} with the binding energy at 457.7 ± 0.1eV and 455.6 ± 0.1eV were formed which is shown in the supporting information. Therefore, the pre-treatment serves as a route to produce a titania surface attractive for the attachment of gold clusters.

The fitting of the peak position of gold and phosphorous with the Shirley background after deposition and post heat treatment is shown in the supplementary information. The initial and

final state effect plays an important role in distinguishing the bulk gold and gold clusters. The initial state effect corresponds to the atomic oxidation state. The final state effect depends on the lifetime of the hole created on the surface and depends on the cluster size. The binding energy shift due to the final effect depends on the size of the gold cluster and also influences the FWHM of the peak in the XP spectrum.[4, 11] The peak position of Au $4f_{7/2}$ after deposition of gold clusters onto the surface of the pre-treated ALD titania is shown in Figure 4.1a and found at 85.1-85.6eV which confirms the presence of un-agglomerated clusters.[1] The FWHM is found around 1.4 – 1.8 which is the same as reported in an earlier publication.[12] The peak position of Au $4f_{7/2}$ component after post heat treatment is shown in figure 4.1b and found at 84.6-85.1eV which is similar but slightly higher compared to the Au_9 clusters deposited on the ALD titania surface with the same pre-treatment conditions where the binding energy is found at 84.6 – 84.8 eV.[9] The peak position of Au $4f_{7/2}$ after post heat treatment shifts towards lower binding energy but this is higher compared to Au_9 clusters.[9] The FWHM remains the same even after the post heat treatment which also supports the conclusion that the gold clusters did not undergo agglomeration. The peak position of phosphorous after deposition is found at 131.9-132.8eV as shown in Figure 4.1c which corresponds to the phosphine ligands attached to the gold clusters.[11] The peak position of phosphorous after post heat treatment is shown in Figure 4.1d and is found at 132.7 - 132.9 eV. The phosphorous peak position is shifted to higher binding energy compared to the as deposited clusters which is interpreted as attachment of the phosphine ligands to the titania surface.[11] It should be noted that the phosphorous peak after heating is only found for higher concentrations (≥ 0.006 mM) of gold clusters and no peak was found for lower gold cluster concentrations (< 0.006 mM). The reason is most likely that the amount of phosphorous was too low to result in a measurable peak.

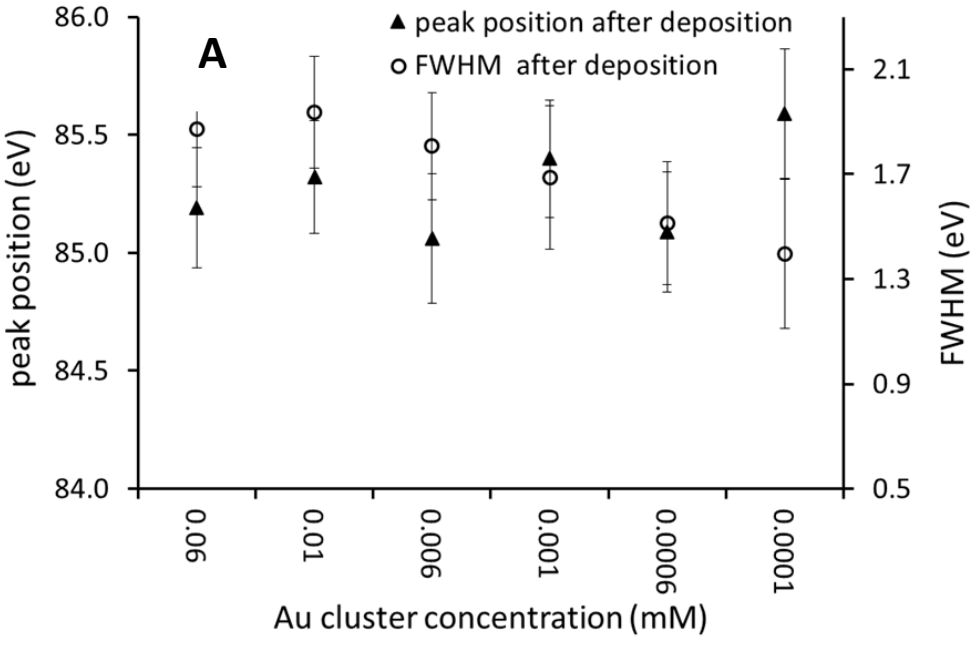

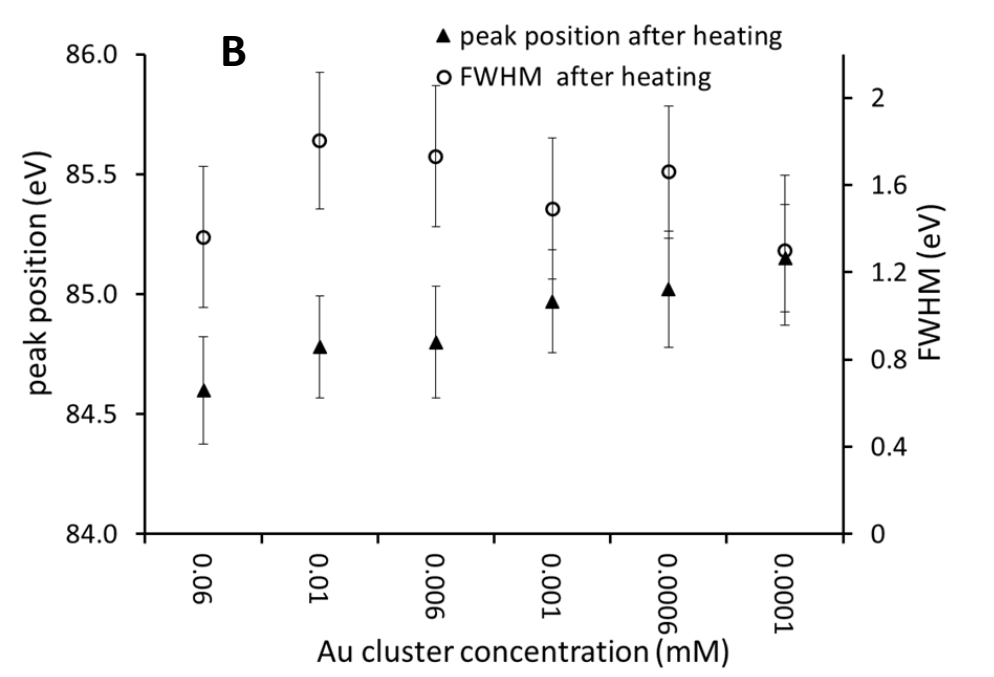
B
peak position after heating
FWHM after heating
86.0
85.5
85.0
84.5
84.0
peak position (eV)
2
1.6
1.2
0.8
0.4
0
FWHM (eV)
0.06
0.01
0.006
0.001
0.0006
0.0001
Au cluster concentration (mM)

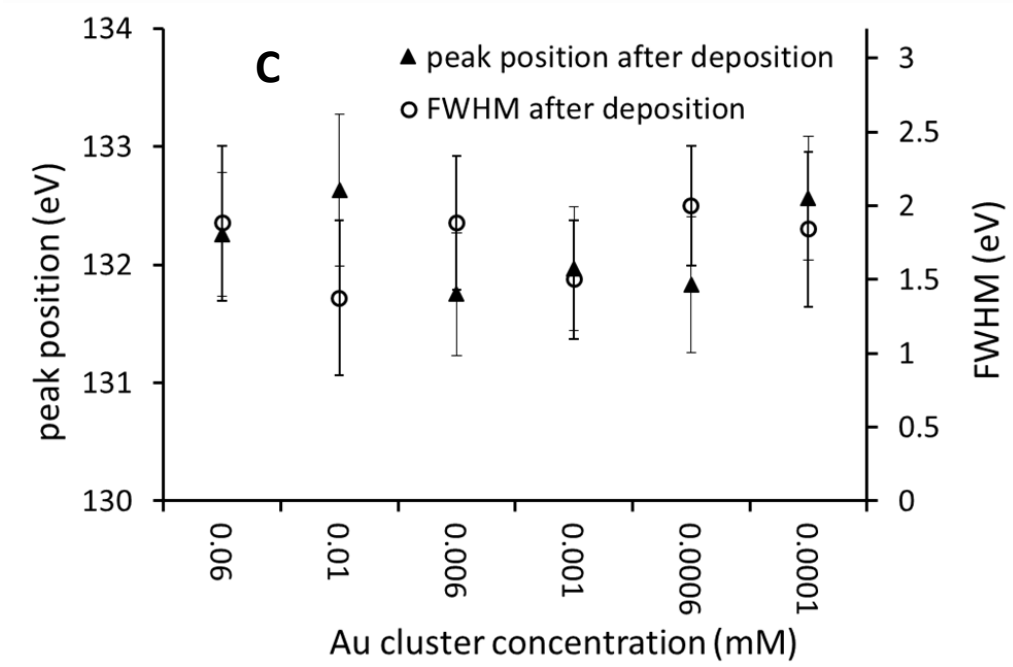
C
peak position after deposition
FWHM after deposition
134
133
132
131
130
peak position (eV)
3
2.5
2
1.5
1
0.5
0
FWHM (eV)
0.06
0.01
0.006
0.001
0.0006
0.0001
Au cluster concentration (mM)

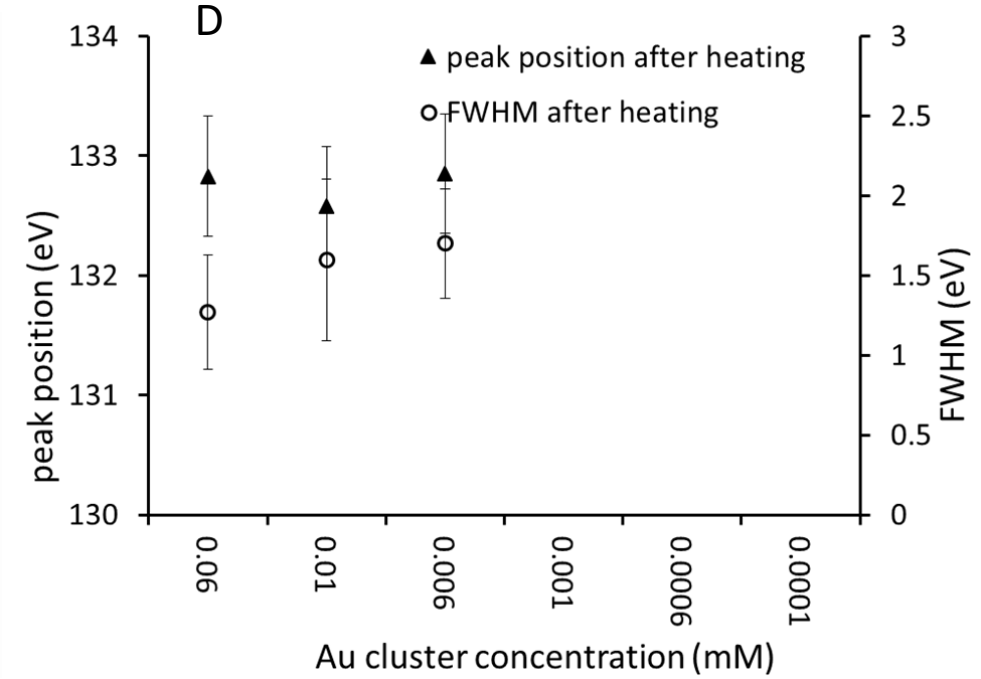

Figure 4. 1: Peak position and FWHM of a) Au after deposition b) Au after post heat treatment c) P after deposition d) P after post heat treatment. The error bar represents the peak fitting uncertainty.

The ratio intensity of phosphorous to gold was found to drop after the post heat treatment which is shown in figure 4.2a. This confirms the removal of ligands from the surface of the clusters and the partial oxidation of the ligands through the attachment onto the titania for higher gold concentrations. For lower concentrations the same mechanism could occur. However, it is also possible that ligands have been removed from the sample surface to a larger degree at lower concentrations of the gold clusters.

Figure 4.2b shows the relative intensity of gold to titania after post heat treatment and it is found that the amount of gold on titania remains the same after deposition and post heat treatment which is another strong indication that there is no agglomeration of clusters after applying the heat treatment. Agglomeration of gold clusters would lead to the formation of larger gold particles which would cause the drop in the intensity of the gold to titania.

The relative intensity of phosphorous to titania shown in figure 4.2c was found to drop after post heat treatment which is a further strong indication that the phosphorous ligands are removed from the gold cluster and attached to the surface of titania for higher concentrations and to a larger degree removed from the titania surface for lower concentrations of gold clusters.

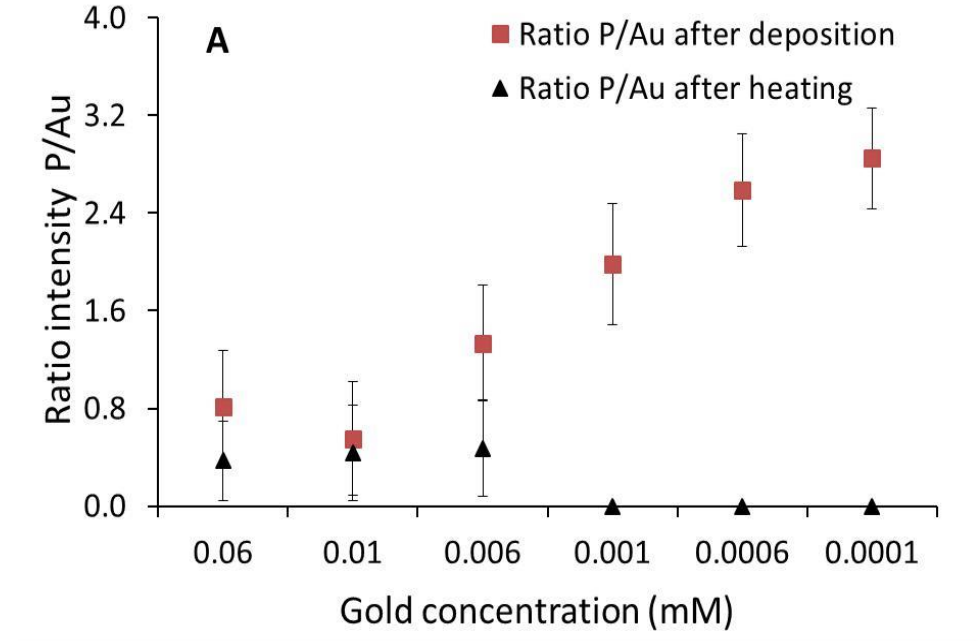
A
Ratio P/Au after deposition
Ratio P/Au after heating
Ratio intensity P/Au
4.0
3.2
2.4
1.6
0.8
0.0
0.06
0.01
0.006
0.001
0.0006
0.0001
Gold concentration (mM)

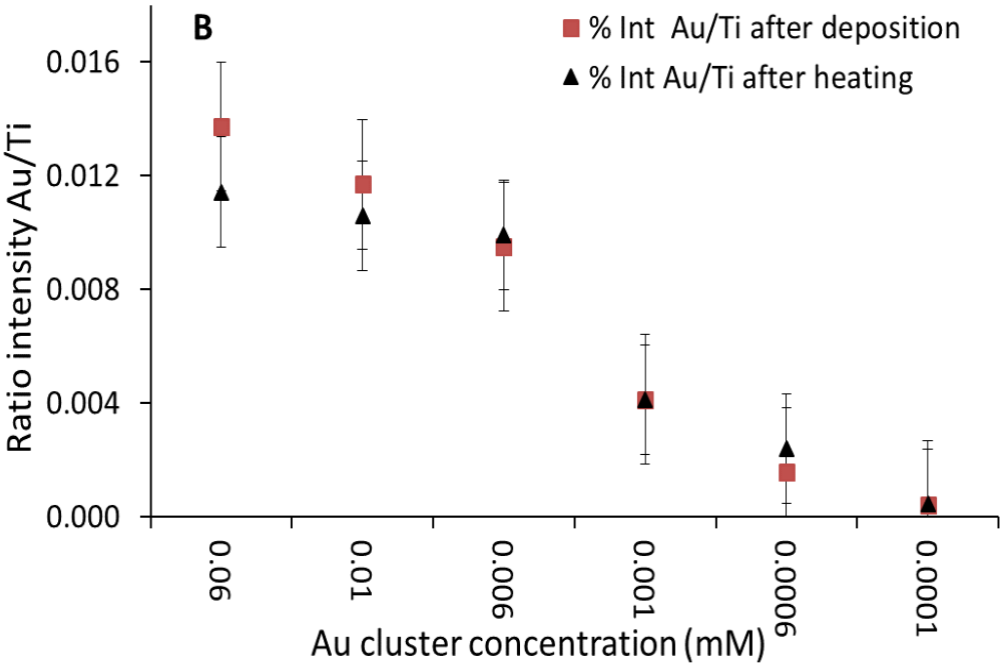
B
% Int Au/Ti after deposition
% Int Au/Ti after heating
Ratio intensity Au/Ti
0.016
0.012
0.008
0.004
0.000
0.06
0.01
0.006
0.001
0.0006
0.0001
Au cluster concentration (mM)

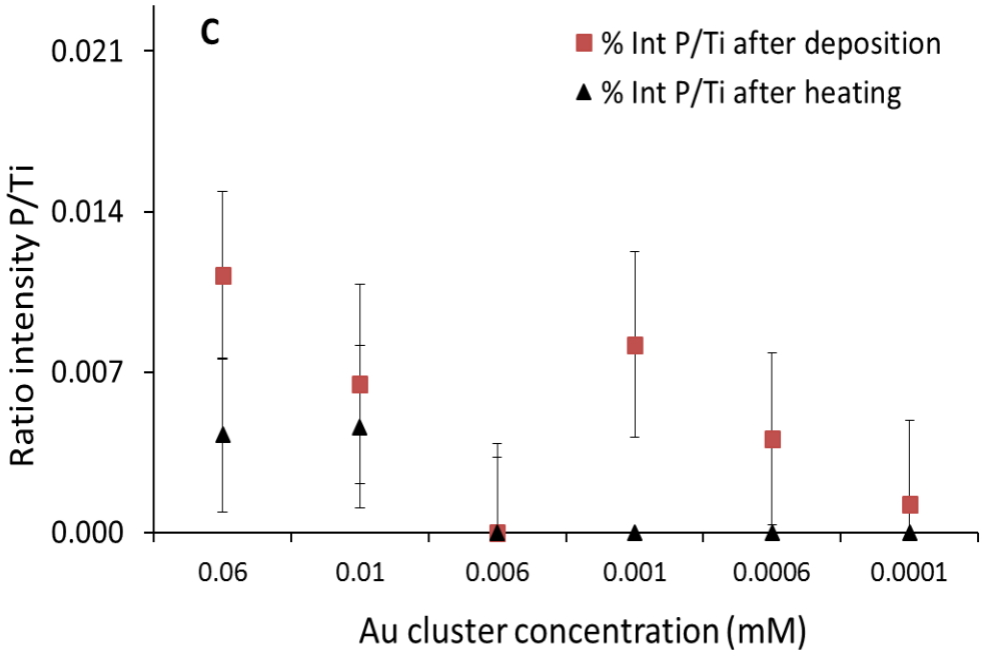

Figure 4.2: XPS ratio intensities after the deposition of gold clusters onto the pre-treated ALD titania and post heat treatment a) % ratio intensity of P to Au b) ratio of Au to Ti c) ratio of P to Ti.

4.3.2. MIES Results

The MIE spectra of samples with different Au_{13} concentrations (0.06 to 0.0001mM) after post heat treatment at 200 °C for 20 minutes are shown in Figure 4.3a. To avoid the variations in the intensity of He* source, the measured raw MIE spectra of all the gold deposited samples after post heat treatment was normalized with the measured MIE spectra after the pre-treated ALD titania. The MIE spectra of the pre-treated ALD titania all have the same shape within the experimental uncertainty.

The three main steps for the MIES spectra analysis of the deposited gold clusters after post heat treatment are as follows:

1) To identify of the number of base spectra required to fit the measured series of MIES spectra determined using the SVD algorithm.
2) To define the meaningful reference spectra.
3) To elucidate the nature of reference spectra.

1. Identification of the number of base spectra required using SVD algorithm:

The number of base spectra is identified using the SVD algorithm mathematical procedure which has been explained in detail previously in.[13-15] The first step defines the number of base spectra required to fit the series of measured MIES spectra shown in Figure 4.3a. It was found that three reference spectra are needed to fit the series of measured MIES spectra as a result of the SVD algorithm.

2. Definition of the meaningful reference spectra:

The number of reference spectra is the same as the number of base spectra, the two main criterions need to be considered in defining the meaningful reference spectra: (i) the reference spectra must be non-negative and (ii) the sum of the weighting factors should be close to unity. The procedure for the second reference spectrum is described briefly in.[9, 16]

3. Elucidation of the reference spectra:

The pre-treated ALD titania sample after post heat treatment was identified as one of the reference spectra which has similar features compared to the previous study of Au_9 clusters.[9] The second reference spectrum is found by comparing the plotting of the weighting factors found as a result of applying the SVD algorithm with the relative intensities of elements from the XPS data analysis. The plotting of XPS relative intensity of Au to Ti with the weighting factors from SVD is shown in figure 4.3c. The weighting factors (β) from MIES analysis for the reference spectrum 2 adapts the same trend as a relative intensity of Au with respect to titania. Therefore, the second reference spectrum corresponds to the presence of the Au_{13} clusters detached from the ligands. The third reference spectrum was identified also as representing titania due to its similarity in shape to reference spectrum 1(titania) and has feature of Au_{13} clusters due to the secondary electron contribution which resulted from the mathematical procedure. It is not possible to eliminate such contribution in case of mathematical procedure. In the previous publication,[9] only one reference spectrum representing titania was found. It is unclear why in the present case a second almost identical reference spectrum for titania is found. However, it must be emphasized that finding a second reference spectrum for titania similar to the first does not affect the data evaluation and interpretation.

The second reference spectrum from the SVD analysis shows strong features at binding energies 4.3, 7.2 and 9.3 eV and it corresponds to density of states of the Au_{13} clusters attached from the ligands. These states can be compared with the states related to Au_9 clusters found in the reference spectra of our previous work investigating Au_9 clusters on identically pre-treated ALD titania. In the previous work, the reference spectra were assigned to (i) titania, (ii) the combination of the presence of Au_9 clusters and phosphine ligands in which the gold has the density of states at binding energy 4.4, 7.3 and 9.4eV [9]. The DOS of the reference spectrum for the Au_{13} clusters appear to be similar to those of the Au_9 clusters but shifted relative to each other in their binding energy by ~0.1 eV which is shown in figure 4.3d. The reason for the similarity of the binding energy might be the similarity in the size of the Au_9 and Au_{13} cluster. A more significant change in the electronic structure could be expected to occur if there is a more significant difference in the size of the clusters. Therefore, future work should investigate smaller clusters (e.g. Au_6) or large clusters (e.g. Au_{25}) which might result in

a larger difference in electronic structure. The reason for the specification of Au_6 or Au_{25} clusters is that these sizes have been syntheized previously by the collaborators.

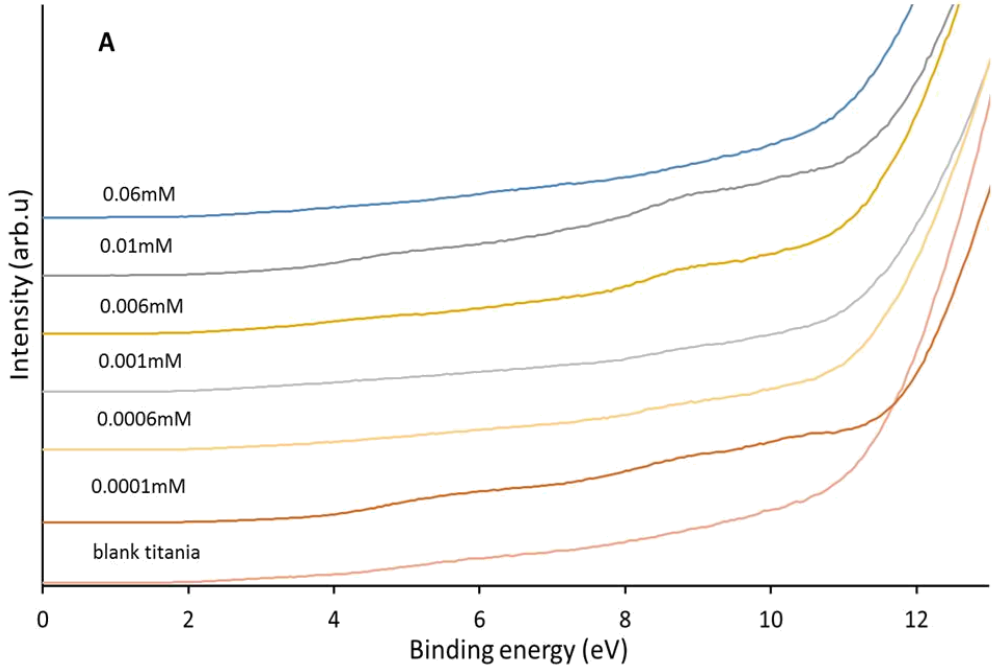

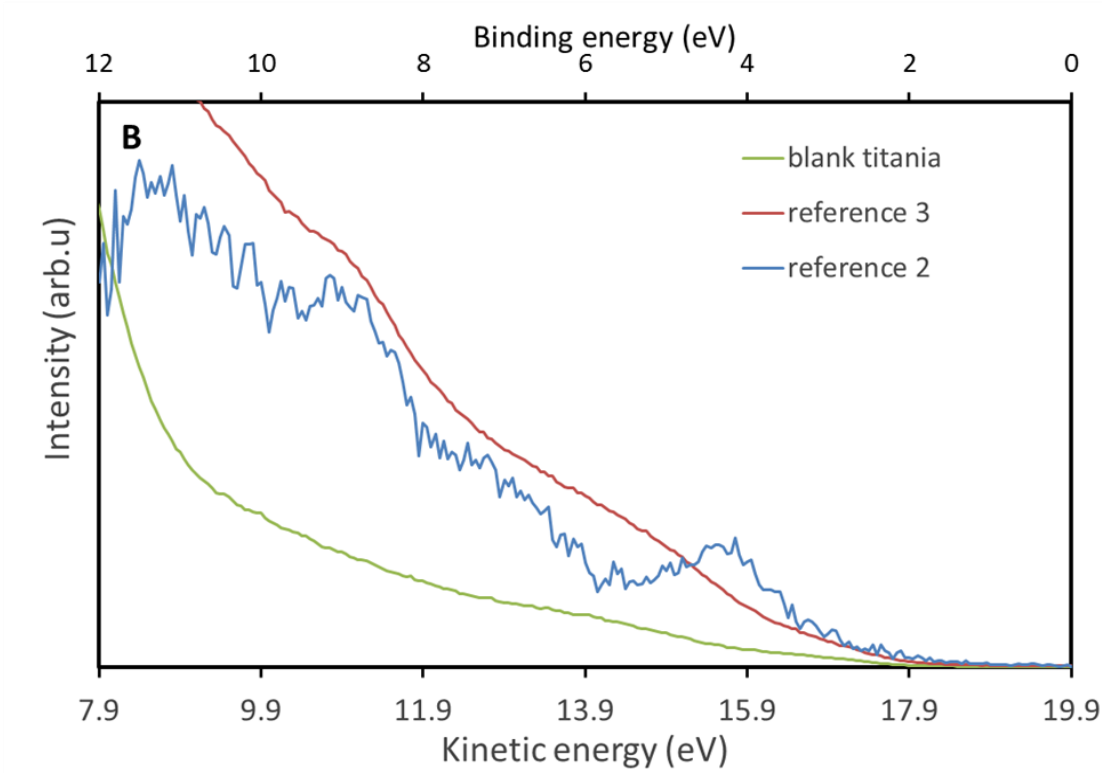

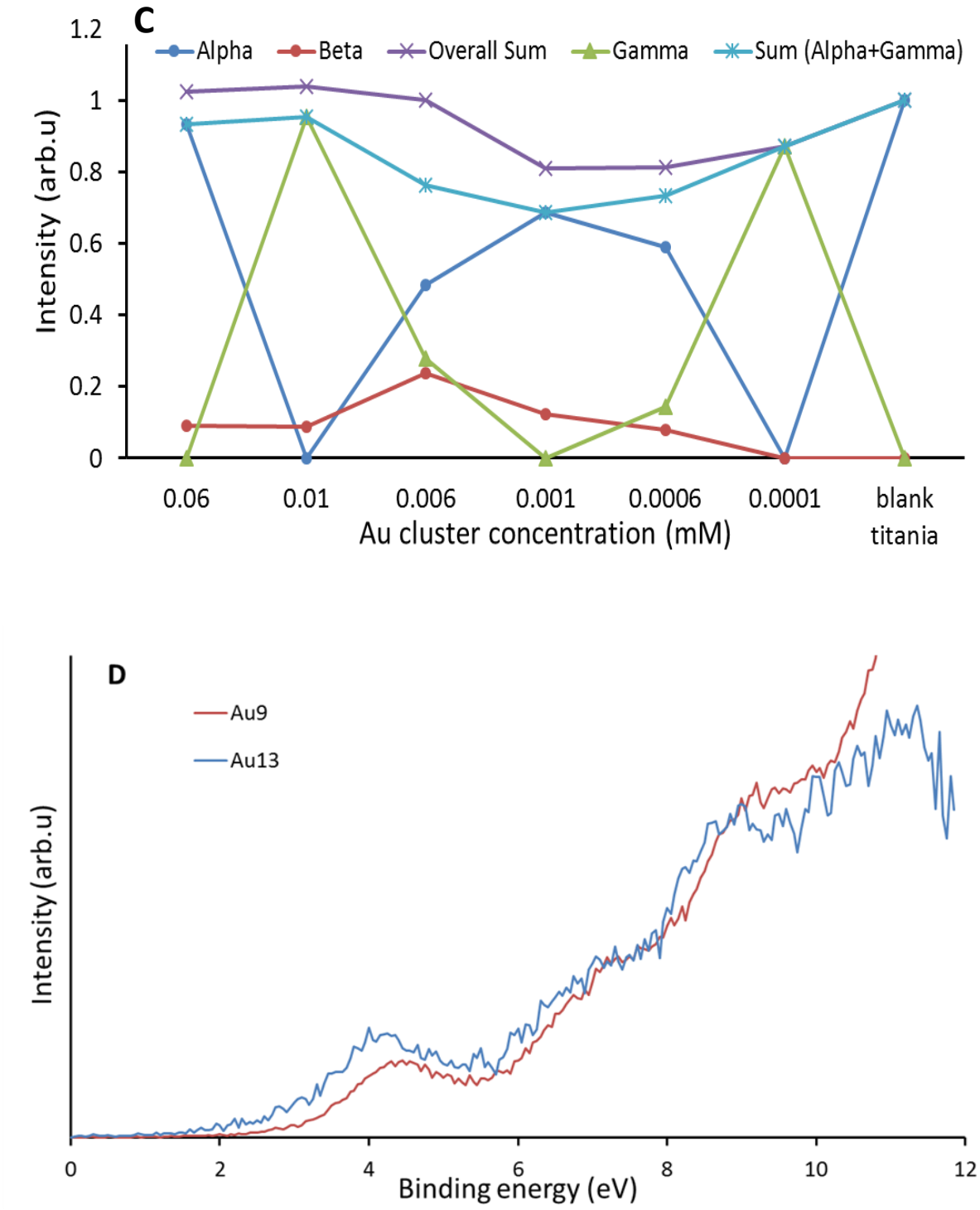

Figure 4.3: a) MIES spectra of various gold concentrations after post heat treatment b) MIES reference spectra after post heat treatment: reference 1 is related to the titania substrate, reference 2 is related to the gold cluster detached from the phosphine ligands, reference 3 has a very similar spectrum as that of the titania and is thus also considered as representing titania c) plotting of the XPS relative intensity of Au to Ti with the weighting factors from the SVD algorithm d) Comparison of the reference spectrum of Au_9 and Au_{13} clusters.

4.4. Conclusion

The atomically precise chemically synthesised triphenylphosphine ligand protected Au_{13} clusters deposited onto the surface of the pre-treated ALD titania was post heated at 200°C for 20 minutes. The electronic structure and the chemical composition of the sample surface was studied using the MIES and XPS. XPS result shows that the Au_{13} clusters deposited onto the pre-treated ALD titania remains un-agglomerated after the post heat treatment and results in the partial removal of phosphine ligands for high gold concentrations while it was completely removed for low gold concentrations. MIES reveals the valence electronic structure of the sample surface. The reference spectra from MIES is associated with the titania substrate and the Au_{13} clusters on the titania surface. The density of states is shifted towards slightly lower binding energies compared to the reference spectra from Au_9 clusters on the titania surfaces. The theoretical calculations of Au_{13} clusters will be of interest same as Au_9 clusters to understand the slight difference between Au_9 and Au_{13} clusters.

4.5. References

1. Sanchez, A.; Abbet, S.; Heiz, U.; Schneider, W. D.; Häkkinen, H.; Barnett, R. N.; Landman, U., When Gold Is Not Noble: Nanoscale Gold Catalysts. *The Journal of Physical Chemistry A* **1999**, *103*, 9573-9578.

2. Schweinberger, F. F., et al., Cluster Size Effects in the Photocatalytic Hydrogen Evolution Reaction. *Journal of the American Chemical Society* **2013**, *135*, 13262-13265.

3. Wahlstrom, E.; Lopez, N.; Schaub, R.; Thostrup, P.; Ronnau, A.; Africh, C.; Laegsgaard, E.; Norskov, J. K.; Besenbacher, F., Bonding of Gold Nanoclusters to Oxygen Vacancies on Rutile Tio2(110). *Phys Rev Lett* **2003**, *90*, 026101.

4. Ruzicka, J.-Y.; Abu Bakar, F.; Hoeck, C.; Adnan, R.; McNicoll, C.; Kemmitt, T.; Cowie, B. C.; Metha, G. F.; Andersson, G. G.; Golovko, V. B., Toward Control of Gold Cluster Aggregation on Tio2 Via Surface Treatments. *The Journal of Physical Chemistry C* **2015**, *119*, 24465-24474.

5. Chen, M. S.; Goodman, D. W., Structure–Activity Relationships in Supported Au Catalysts. *Catalysis Today* **2006**, *111*, 22-33.

6. Valden, M.; Lai, X.; Goodman, D. W., Onset of Catalytic Activity of Gold Clusters on Titania with the Appearance of Nonmetallic Properties. *Science* **1998**, *281*, 1647-1650.

7. Heiz, U.; Vanolli, F.; Sanchez, A.; Schneider, W. D., Size-Dependent Molecular Dissociation on Mass-Selected, Supported Metal Clusters. *Journal of the American Chemical Society* **1998**, *120*, 9668-9671.

8. Wörz, A. S.; Judai, K.; Abbet, S.; Heiz, U., Cluster Size-Dependent Mechanisms of the Co + No Reaction on Small Pdn ($N \leq 30$) Clusters on Oxide Surfaces. *Journal of the American Chemical Society* **2003**, *125*, 7964-7970.

9. Krishnan, G.; Al Qahtani, H. S.; Li, J.; Yin, Y.; Eom, N.; Golovko, V. B.; Metha, G. F.; Andersson, G. G., Investigation of Ligand-Stabilized Gold Clusters on Defect-Rich Titania. *The Journal of Physical Chemistry C* **2017**, *121*, 28007-28016.

10. Shirley, D. A., High-Resolution X-Ray Photoemission Spectrum of the Valence Bands of Gold. *Physical Review B* **1972**, *5*, 4709-4714.

11. Anderson, D. P.; Alvino, J. F.; Gentleman, A.; Qahtani, H. A.; Thomsen, L.; Polson, M. I.; Metha, G. F.; Golovko, V. B.; Andersson, G. G., Chemically-Synthesised, Atomically-Precise Gold Clusters Deposited and Activated on Titania. *Phys Chem Chem Phys* **2013**, *15*, 3917-29.

12. Anderson, D. P., et al., Chemically Synthesised Atomically Precise Gold Clusters Deposited and Activated on Titania. Part Ii. *Phys Chem Chem Phys* **2013**, *15*, 14806-13.

13. Bennett, T.; Adnan, R. H.; Alvino, J. F.; Golovko, V.; Andersson, G. G.; Metha, G. F., Identification of the Vibrational Modes in the Far-Infrared Spectra of Ruthenium Carbonyl Clusters and the Effect of Gold Substitution. *Inorganic chemistry* **2014**, *53*, 4340-4349.

14. Chambers, B. A.; Neumann, C.; Turchanin, A.; Gibson, C. T.; Andersson, G. G., The Direct Measurement of the Electronic Density of States of Graphene Using Metastable Induced Electron Spectroscopy. *2D Materials* **2017**, *4*, 025068.

15. Höfft, O.; Bahr, S.; Himmerlich, M.; Krischok, S.; Schaefer, J. A.; Kempter, V., Electronic Structure of the Surface of the Ionic Liquid [Emim][Tf2n] Studied by Metastable Impact Electron Spectroscopy (Mies), Ups, and Xps. *Langmuir* **2006**, *22*, 7120-7123.

16. Andersson, G. G., et al., Phosphine-Stabilised Au(9) Clusters Interacting with Titania and Silica Surfaces: The First Evidence for the Density of States Signature of the Support-Immobilised Cluster. *J Chem Phys* **2014**, *141*, 014702.

Chapter 5

5.1. Conclusions

The chemically synthesized atomically precise phosphine stabilized Au_n (n=9,13) clusters deposited onto the pre-treated ALD titania surface were post heated at 200 ºC for 20 minutes. The pre-treatment involves the heating and subsequent sputtering. The electronic structure and the chemical composition of the sample surface after the post heat treatment was investigated using XPS and MIES. XPS was used to determine the chemical composition of the sample surface. The XPS results revealed that the Au_9 clusters deposited on the pre-treated ALD titania are most likely not agglomerated after the post heat treatment but found at a binding energy slightly lower than observed previously. The triphenylphosphine ligands are completely removed from the Au_9 surface and found oxidized onto the ALD titania surface. In the case of Au_{13} clusters deposited onto the pre-treated ALD titania remains un-agglomerated after the post heat treatment and results in the partial removal of phosphine ligands for high gold concentrations while it was completely removed for low gold concentrations. An important outcome of the present work is that defects introduced into the ALD titania surface via sputtering and heating strongly reduces the agglomeration of the Au clusters adsorbed to the surface. In our previous work ligand stabilized showed a significant degree of agglomeration when deposited onto defect poor ALD Titania surfaces.

The MIES results for Au_9 clusters onto the ALD titania revealed that two reference spectra are required to explain the electronic structure of the sample. One reference spectrum is related to the titania substrate while the second spectrum is related to the presence of the Au clusters and the ligands removed from the cluster cores. The interpretation of the reference spectrum of the Au clusters shows that the Au states which can be clearly identified in the MIE spectra have their lowest binding energy at approximately 1.8 eV. The observed DOS of Au_9 are comparable to those calculated by DFT. In case of Au_{13} clusters on the surface of the ALD Titania, the reference spectra from MIES is associated with the Titania substrate and the Au_{13} clusters on the Titania surface. The DOS of the reference spectrum for the Au_{13} clusters appear to be similar to those of the Au_9 clusters but shifted relative to each other in their binding energy by ~0.1 eV which might be because of the similarity in the size of the Au_9 and Au_{13} cluster. Also, theoretical calculations are ongoing for the Au_{13} clusters on the titania surface which helps with the understanding of the small difference in the DOS between the Au_9 and Au_{13} clusters. The

future work will be focused on investigating the smaller clusters (e.g. Au_6) or large clusters (e.g. Au_{25}) following the same method which might result in a larger difference in electronic structure.